# An inter-laboratory comparison of aerosol inorganic ion measurements by Ion Chromatography: implications for aerosol pH estimate

Jingsha Xu[1], Shaojie Song[2], Roy M. Harrison[1], Congbo Song[1], Lianfang Wei[3], Qiang Zhang[4], Yele Sun[3], Lu Lei[3], Chao Zhang[5], Xiaohong Yao[5, 6], Dihui Chen[5], Weijun Li[7], Miaomiao Wu[7], Hezhong Tian[8], Lining Luo[8], Shengrui Tong[9], Weiran Li[9], Junling Wang[10], Guoliang Shi[11], Yanqi Huangfu[11], Yingze Tian[11], Baozhu Ge[3], Shaoli Su[12], Chao Peng[12], Yang Chen[12], Fumo Yang[13], Aleksandra Mihajlidi-Zelić[14], Dragana Đorđević[14], Stefan J. Swift[15], Imogen Andrews[15], Jacqueline F. Hamilton[15], Ye Sun[16], Agung Kramawijaya[1], Jinxiu Han[1], Supattarachai Saksakulkrai[1], Clarissa Baldo[1], Siqi Hou[1], Feixue Zheng[17], Kaspar R. Daellenbach[17], Chao Yan[17], Yongchun Liu[17], Markku Kulmala[17], Pingqing Fu[4], Zongbo Shi*[1]

1 School of Geography Earth and Environmental Science, University of Birmingham, Birmingham, B15 2TT, UK

2 School of Engineering and Applied Sciences, Harvard University, Cambridge, MA 02138, USA

3 State Key Laboratory of Atmospheric Boundary Layer Physics and Atmospheric Chemistry, Institute of Atmospheric Physics, Chinese Academy of Sciences, Beijing, 100029, China

4 Institute of Surface-Earth System Science, Tianjin University, Tianjin, 300072, China

5 Frontiers Science Center for Deep Ocean Multispheres and Earth System, and Key Laboratory of Marine Environment and Ecology, Ministry of Education of China, Ocean University of China, Qingdao 266100, China

6 Laboratory for Marine Ecology and Environmental Sciences, Qingdao National Laboratory for Marine Science and Technology, Qingdao 266071, China

7 Department of Atmospheric Sciences, School of Earth Sciences, Zhejiang University, Hangzhou, 310027, China

8 Center for Atmospheric Environmental Studies, Beijing Normal University, Beijing, 100875, China

9 State Key Laboratory of Structural Chemistry of Unstable and Stable Species, Institute of Chemistry, Chinese Academy of Sciences, Beijing, 100190, China

10 School of Environment, Tsinghua University, Beijing, 100084, China

11 State Environmental Protection Key Laboratory of Urban Ambient Air Particulate Matter Pollution Prevention and Control, Center for Urban Transport Emission Research, College of Environmental Science and Engineering, Nankai University, Tianjin, 300350, China

12 Research Center for Atmospheric Environment, Chongqing Institute of Green and Intelligent Technology, Chinese Academy of Sciences, Chongqing, 400714, China

13 Department of Environmental Science and Engineering, Sichuan University, Chengdu, 610065, China

14 Centre of Excellence in Environmental Chemistry and Engineering – ICTM, University of Belgrade, Njegoševa 12 (Studentski trg 14–16), Belgrade, Serbia

15 Department of Chemistry, University of York, York, YO10 5DD, UK

16 School of Space and Environment, Beihang University, Beijing, 100191, China

17 Beijing Advanced Innovation Center for Soft Matter Science and Engineering, Beijing University of Chemical Technology, Beijing, 100029, China

Correspondence: Zongbo Shi (Z.Shi@bham.ac.uk)

**ABSTRACT**

Water soluble inorganic ions such as ammonium, nitrate, and sulfate are major components of fine aerosols in the atmosphere and are widely used in the estimation of aerosol acidity. However, different experimental practices and instrumentation may lead to uncertainties in ion concentrations. Here, an inter-comparison experiment was conducted in 10 different laboratories (labs) to investigate the consistency of inorganic ion concentrations and resultant aerosol acidity estimates using the same set of aerosol filter samples. The results mostly exhibited good agreement for major ions $Cl^-$, $SO_4^{2-}$, $NO_3^-$, $NH_4^+$ and $K^+$. However, $F^-$, $Mg^{2+}$ and $Ca^{2+}$ were observed with more variations across the different labs. The Aerosol Chemical Speciation Monitor (ACSM) data of non-refractory $SO_4^{2-}$, $NO_3^-$, $NH_4^+$ generally correlated very well with the filter analysis based data in our study, but the absolute concentrations differ by up to 42%. $Cl^-$ from the two methods are correlated but the concentration differ by more than a factor of three. The analyses of certified reference materials (CRMs) generally showed good detection accuracy (DA) of all ions in all the labs, the majority of which ranged between 90% and 110%. The DA was also used to correct the ion concentrations to showcase the importance of using CRM for calibration check and quality control. Better agreements were found for $Cl^-$, $SO_4^{2-}$, $NO_3^-$, $NH_4^+$ and $K^+$ across the labs after their concentrations were corrected with DA; the coefficient of variation (CV) of $Cl^-$, $SO_4^{2-}$, $NO_3^-$, $NH_4^+$ and $K^+$ decreased 1.7%, 3.4%, 3.4%, 1.2% and 2.6%, respectively, after DA correction. We found that the ratio of anion to cation equivalent concentrations (AE/CE) and Ion balance (anions − cations) are not a good indicator for aerosol acidity estimates, as the results in different labs did not agree well with each other. In situ aerosol pH calculated from the ISORROPIA-II thermodynamic equilibrium model with measured ion and ammonia concentrations showed a similar trend and good agreement across the 10 labs. Our results indicate that although there are important uncertainties in aerosol ion concentration measurements, the estimated aerosol pH from the ISORROPIA-II model is more consistent.

**Keywords:** $PM_{2.5}$, inorganic ions, aerosol acidity, ion balance, thermodynamic model

62

## 1.    INTRODUCTION

Water-soluble inorganic ions (WSII), consisting of $F^-$, $Cl^-$, $NO_2^-$, $NO_3^-$, $SO_4^{2-}$, $NH_4^+$, $Na^+$, $K^+$, $Mg^{2+}$ and $Ca^{2+}$, are a major component of atmospheric aerosols and can contribute up to 77% of $PM_{2.5}$ (particulate matter with aerodynamic diameter $\leq 2.5\ \mu m$) mass (Xu et al., 2019a). Secondary inorganic aerosols (SIA) including sulfate, nitrate and ammonium (SNA) often dominate water-soluble ionic species in $PM_{2.5}$, and were reported to account for more than 90% of WSII in Sichuan, China (Tian et al., 2017). In Beijing, the average SNA concentrations can range from $4.2 \pm 2.9\ \mu g/m^3$ in non-haze days to $85.9 \pm 22.4\ \mu g/m^3$ in heavily polluted days, and contribute 15%-49% of $PM_{2.5}$ (Li et al., 2016). SNA can greatly influence air pollution, visibility, aerosol acidity and hygroscopicity, which are driving factors affecting aerosol-phase pH and chemistry and the uptake of gaseous species by particles (Shon et al., 2012; Xue et al., 2011; Zhang et al., 2019). Hence, the study of WSII is of great interest due to their adverse impacts.

WSII in aerosols were reported to be analyzed by multiple techniques such as $Cl^-$ by spectrophotometry, and $Ca^{2+}$ and $Mg^{2+}$ by flame atomic absorption in the early 1980s (Harrison and Pio, 1983). However, previous methods were time-consuming as WSII were analyzed by different techniques separately. Ion chromatography (IC), which was first introduced in 1975 (Buchberger, 2001), was applied in many studies for routine measurement of atmospheric WSII due to its fast, accurate and sensitive determination in a single run (Heckenberg and Haddad, 1984; Baltensperger and Hertz, 1985). IC can be coupled with diverse detection techniques for ion analysis, such as suppressed conductivity, UV-VIS absorbance, amperometry, potentiometry, mass spectrometry, etc. (Buchberger, 2001). It has been used in various atmospheric studies for many years and is still widely applied at present, such as in the investigation of WSII in size-segregated aerosols (Li et al., 2013; Zhao et al., 2011; Đorđević et al., 2012), fine aerosols (Fan et al., 2017; He et al., 2017; Liu et al.,

2017a) and coarse aerosols (Li et al., 2014; Guo et al., 2011; Mkoma et al., 2009). IC can also be used for the determination of both water soluble organic and inorganic ions (Yu et al., 2004; Karthikeyan and Balasubramanian, 2006).

Aerosol ion concentrations can also be measured by online methods such as the Aerosol Chemical Speciation Monitor (ACSM) or Aerosol Mass Spectrometer (AMS) (Ng et al., 2011; Sun et al., 2012). During the recent Atmospheric Pollution and Human Health in a Chinese Megacity (APHH-China) campaigns (Shi et al., 2019), we observed important discrepancies between offline aerosol IC observations from different labs and between online AMS and offline IC methods. This prompted us to carry out this intercomparison exercise.

The IC method had been validated by a common reference standard - NIST SRM 1648 (urban particulate matter) and the results for Na, K, S and $NH_4^+$ were compared with those from other suitable alternative analytical techniques such as AAS, UV-VIS and PIXE in previous studies (Karthikeyan and Balasubramanian, 2006). However, to the best of our knowledge, no investigation has been conducted to compare the results of different laboratories (labs) for such an important and widely used simple technique.

The aim of this work is to 1) examine the consistency of ion concentrations measured by various labs and by ACSM, 2) explore the impact of the inter-lab variability in ion concentration measurements on aerosol acidity estimates, and 3) provide recommendations for improving future WSII analysis by IC.

## 2. EXPERIMENTAL

### 2.1 Participating Laboratories

Ten laboratories from China, United Kingdom and Serbia were invited to take part in the inter-laboratory comparison of atmospheric inorganic ions, which are listed as follows: University of Birmingham; University of York; University of Belgrade; Zhejiang University; Nankai University;

112    Ocean University of China; Beijing Normal University; Chongqing Institute of Green and Intelligent

113    Technology, Chinese Academy of Sciences; Institute of Chemistry, Chinese Academy of Sciences;

114    Institute of Atmospheric Physics, Chinese Academy of Sciences. The participating laboratories were

115    randomly coded from Lab-1 to Lab-10 and not related to the above order.

116

## 117    2.2    Sample and Data Collection

118    Eight daily $PM_{2.5}$ samples were collected on quartz filters (total area: $406.5cm^2$) from $16^{th}$-$23^{rd}$

119    January 2019 by a high-volume air sampler (1.13 $m^3$ $min^{-1}$; Tisch Environmental Inc., USA) at an

120    urban site, located at the Institute of Atmospheric Physics (IAP) of the Chinese Academy of Sciences

121    in Beijing, China. The sampling site (116.39E, 39.98N) is located between the North Third Ring Road

122    and North Fourth Ring Road, and approximately 200 m from the G6 Highway. It is 8 m above the

123    ground and surrounded by high-density roads and buildings; detailed information regarding the

124    sampling site can be found elsewhere (Shi et al., 2019). Apart from the aerosol samples, 5 field blank

125    filters were also collected in the same manner with the pump off. All ion concentrations in this study

126    were corrected by the values obtained from field blanks. Hourly $PM_{2.5}$ mass concentrations were

127    obtained from a nearby Olympic Park station, the China National Environmental Monitoring Network

128    (CNEM) website. Shi et al. (2019) showed that the $PM_{2.5}$ data at this station are close to those

129    observed at IAP during the APHH-China campaigns. The close observed $PM_{2.5}$ concentrations at

130    different air quality stations in Beijing provide further reassurance of the representability of the

131    observed concentration at Olympic Park. The original hourly data was averaged to 24 h for better

132    comparison.

133

134    An Aerodyne Time-of-Flight Aerosol Chemical Speciation Monitor (ToF-ACSM) with a $PM_{2.5}$

135    aerodynamic lens was also deployed on the same roof of the building at IAP for real-time

136    measurements of non-refractory (NR) chemical species (Organics, $Cl^-$, $NO_3^-$, $SO_4^{2-}$ and $NH_4^+$) in

137    PM$_{2.5}$ (NR-PM$_{2.5}$) with 2 min time resolution (Sun et al., 2020). Another ToF-ACSM was also used

138    to measure the PM$_{2.5}$-associated non-refractory chemical species at the Beijing University of

139    Chemical Technology (BUCT), which is located at the west third-Ring Road of Beijing and

140    approximately 10 km away from the sampling location of IAP. The collection efficiencies (CE)

141    applied for the ACSM at IAP and BUCT were different. For IAP, a capture vaporizer was used, and

142    the CE was assumed to be close to 1 (Sun et al., 2020). For BUCT, a standard vaporizer was applied

143    with a composition- and acidity-dependent CE calculated according to Middlebrook et al. (2012).

144    Details regarding quality control of the ACSM at IAP and BUCT can be found elsewhere (Sun et al.,

145    2020; Liu et al., 2020). The concentrations of non-refractory species were calculated from mass

146    spectra using a fragmentation table (Allan et al., 2004). The ToF-ACSM data were then averaged to

147    24h for a comparison with those from filter analysis in our study. Note that the ToF-ACSM data at

148    IAP on 19th and 20th and data at BUCT on 17th and 18th are excluded from the comparison due to the

149    maintenance of the instrument. An ammonia analyzer (DLT‐100, Los Gatos Research LGR, USA)

150    which applies a unique laser absorption technology called off-axis integrated cavity output

151    spectroscopy was used for the ambient NH$_3$ measurements. It has a precision of 0.2 ppb and the

152    original data with 5 min intervals were averaged to 24 h for the calculation of aerosol pH. More

153    information on NH$_3$ measurement can be found elsewhere (Ge et al., 2019).

154

155    **2.3    Sample Analysis**

156    Filter cuts of 5cm$^2$ and 6cm$^2$ from the same set of samples were used for extraction in 10 labs. Filters

157    were extracted ultrasonically for 30 minutes with 10 ml ultrapure water in all laboratories and then

158    filtered before IC analysis. The instrument details are given in Table 1 and the extraction details

159    including purity of ultrapure water, model/power of ultrasonicator, type of syringe filter and vials that

160    used for analysis are provided in Table S1. In total, 9 ionic species were reported: F$^-$, Cl$^-$, SO$_4^{2-}$, NO$_3^-$,

161    Na$^+$, NH$_4^+$, K$^+$, Mg$^{2+}$ and Ca$^{2+}$. Other ions including Br$^-$, NO$_2^-$, PO$_4^{3-}$ and Li$^+$ were not included due

162 to their relatively low concentrations in aerosol samples. The calibration detail and QA/QC

163 procedures are provided in Table S2.

164

165 Certified reference materials (CRM) were also determined for quality control. CRM for cations

166 (CRM-C, Multi Cation Standard 1 for IC, Sigma-Aldrich) contains 200mg/L $Na^+$, 200mg/L $K^+$,

167 50mg/L $Li^+$, 200mg/L $Mg^{2+}$, 1000mg/L $Ca^{2+}$ and 400mg/L $NH_4^+$. CRM for anion (CRM-A, Multi

168 Anion Standard 1 for IC, Sigma-Aldrich) contains 3mg/L $F^-$, 10mg/L $Cl^-$, 20mg/L $Br^-$, 20mg/L $NO_3^-$,

169 20mg/L $SO_4^{2-}$ and 30mg/L $PO_4^{3-}$. CRM-C and CRM-A were diluted 180 and 6 times, respectively.

170 20mL of the diluted CRM solutions were marked as unknown solutions and sent along with the

171 aerosol samples to each lab for analysis. All CRM solutions were measured by each lab as unknown

172 samples. All filters and solutions were kept frozen during transportation to prevent any loss due to

173 volatilization.

174 **Table 1.** Summary of instrument and method details in 10 laboratories.

| Lab No. | Instrument model (Ion Chromatograph) | | Columns & suppressor | | Eluent | |
|---|---|---|---|---|---|---|
| | Anions | Cations | Anions | Cations | Anions | Cations |
| 1 | Dionex AQUNION-1100 | Dionex AQUNION-1100 | IonPac™ AS11-HC separation column; IonPac™ AG11-HC guard column; suppressor ASRS 300 | IonPac™ CS12A separation column; IonPac™ CG12A guard column; suppressor CSRS 300; | 30 mM KOH; 1.0 ml/min. | 20 mM methansulfonic acid; 1.0 ml/min. |
| 2 | Dionex ICS-1100 | Dionex ICS-1100 | IonPac™ AS11-HC separation column; IonPac™ AG11-HC guard column; suppressor ASRS 500 | IonPac™ CS12A separation column; IonPac™ CG12A guard column; suppressor CSRS 500 | KOH with gradient variation from 0 to 30 mM; 0.38 ml/min. | 15 mM methansulfonic acid; 0.25 ml/min |
| 3 | Dionex ICS-600 | Dionex ICS-600 | IonPac™ AS11-HC separation column; IonPac™ AG11-HC guard column; suppressor ASRS 300 | IonPac™ CS12A separation column; IonPac™ CG12A guard column; suppressor CSRS 300 | 20 mM KOH; 1.0 ml/min. | 20 mM methansulfonic acid; 1.0 ml/min |
| 4 | Dionex 600 | Dionex ICS 2100 | IonPac™ AS11 separation column; IonPac™ AG11 guard column; suppressor ASRS 300 | IonPac™ CS12A separation column; IonPac™ CG12A guard column; suppressor CSRS 300 | 30 mM KOH; 1.0 ml/min | 20 mM methansulfonic acid; 1.0 ml/min |
| 5 | Ion Chromotragraph (ECO) | Ion Chromotragraph (ECO) | Metrosep A5-150 separation column; Metrosep A SUPP 4/5 Guard/4.0 guard column; suppressor MSM | Metrosep C4-150 separation column | 3.2 mM $Na_2CO_3$-1.0mM $NaHCO_3$; 0.7 ml/min | 1.7 mM nitric acid - 0.7mM dipicolinic acid; 0.9 ml/min |
| 6 | Metrohm (940 Professional IC Vario) | Metrohm (940 Professional IC Vario) | Metrohm A SUPP 5-250 separation column; Metrohm A SUPP 10-250 guard column; suppressor MSM-A Rotor | METROSEP C6-150 separation column; Metrohm C4 guard column | 3.2 mM $Na_2CO_3$-1.0mM $NaHCO_3$; 0.7 ml/min | 1.7 mM nitric acid - 1.7mM dipicolinic acid; 0.9 ml/min |

| | | | | | | |
|---|---|---|---|---|---|---|
| 7 | Dionex ICS600 | Dionex ICS600 | IonPac™ AS11-HC separation column; IonPac™ AG11-HC guard column; suppressor ASRS | IonPac™ CS12A separation column; IonPac™ CG12A guard column; suppressor CSRS | 30 mM KOH; 1ml/min | 20 mM methansulfonic acid; 1.0 ml/min |
| 8 | Dionex ICS-900 | Dionex ICS-900 | IonPac™ AS14 separation column; IonPac™ AG14 guard column; suppressor Dionex CCRS 500 | IonPac™ CS12A separation column; IonPac™ CG12A guard column; suppressor Dionex CCRS 500 | 3.5 mM $Na_2CO_3$-1.0mM $NaHCO_3$; 1.2 ml/min | 20 mM methansulfonic acid; 1.0 ml/min |
| 9 | Dionex ICS-1100 | Dionex ICS-1100 | IonPac™ RFICTM AS14A separation column; IonPac™ RFICTM AG14A Guard column | IonPac™ RFICTM CS12A separation column; IonPac™ RFICTM CG12A Guard column | 8.0 mM $Na_2CO_3$-1.0mM $NaHCO_3$; 1.0 ml/min | 20 mM methansulfonic acid; 1.0 ml/min |
| 10 | Dionex ICS-2100 | Dionex INTEGRION HPIC | IonPac™ AS15 separation column; IonPac™ AG15 guard column; suppressor ADRS 600 | IonPac™ CS12A separation column; IonPac™ CG12A guard column; suppressor CERS 500; | 38mM KOH; 0.3 ml/min. | 20 mM methansulfonic acid; 1.0 ml/min. |

175

## 2.4    Coefficient of Divergence Analysis

In order to investigate the differences of ionic concentrations measured by different labs, the Pearson's correlation coefficient (R) and the coefficient of divergence (COD) were applied. COD is a parameter to evaluate the degree of uniformity or divergence of two datasets. COD and R were computed for $Lab_j$/Lab-Median pairs, of which $Lab_j$ indicates the results of each lab and Lab-Median represents the median values of 10 labs. Median values are chosen here to better represent the theoretical true concentrations of the ions, as there are some outliers in some labs, and the averages may be less representative. The results of COD and R were also computed for $Lab_j$/Lab-Mean, $Lab_j$/Lab-Upper and $Lab_j$/Lab-Lower pairs (Supplemental Information Fig. S1-S3), where Lab-Mean, Lab-Upper and Lab-Lower represent the mean value, upper values (84% percentile) and lower values (16% percentile) of ion concentrations measured by 10 labs. COD of ionic concentrations of two datasets is determined as follows:

$$COD_{jk} = \sqrt{\frac{1}{P}\sum_{i=1}^{P}(\frac{X_{ij}-X_{ik}}{X_{ij}+X_{ik}})^2} \qquad (1)$$

where j represents the ion concentrations measured by an individual lab-j, k stands for the median ion concentrations of 10 labs, P is the number of samples. $X_{ij}$ and $X_{ik}$ represent the concentration of ion i measured by lab-j and the median concentration of ion i measured by 10 labs, respectively. COD value equal to 0 implies no difference between two datasets, while a COD of 1 means absolute heterogeneity and maximum difference between two datasets (Liu et al., 2017c). A COD value of 0.2 is applied as an indicator for similarity and variability (Krudysz et al., 2008). A higher COD (>0.2) implies variability between two datasets, while lower COD (<0.2) indicates similarity between them. Overall, lower COD (<0.2) and higher R (>0.8) of the lab suggest the similar variation pattern and similar ion concentrations of this lab with the median values of 10 labs.

9

## 2.5    ISORROPIA-II

ISORROPIA-II is a thermodynamic equilibrium model for predicting the composition and physical state of atmospheric inorganic aerosols (available at http://isorropia.eas.gatech.edu) (Fountoukis and Nenes, 2007). It was applied in this study to calculate the aerosol water content (AWC) and pH. Aerosol pH in this study (pH$_i$) was defined as the molality-based hydrogen ion activity on a logarithmic scale, calculated applying the following equation (Jia et al., 2018; Song et al., 2019):

$$pH_i = -\log_{10}\left(a_{H^+_{(aq)}}\right) = -\log_{10}\left(m_{H^+_{(aq)}}\gamma_{H^+_{(aq)}}/m^\Theta\right) \tag{2}$$

where $a_{H^+_{(aq)}}$ represents hydrogen ion activity in aqueous solution, $H^+_{(aq)}$. $m_{H^+_{(aq)}}$ and $\gamma_{H^+_{(aq)}}$ represent the molality and the molality-based activity coefficient of $H^+_{(aq)}$, respectively. $m^\Theta$ is the standard molality (1 mol kg$^{-1}$). Model inputs include aerosol-phase Cl$^-$, SO$_4^{2-}$, NO$_3^-$, Na$^+$, NH$_4^+$, K$^+$, Mg$^{2+}$, Ca$^{2+}$ and gas-phase NH$_3$ concentrations, along with daily averaged temperature and relative humidity (Table S3). In this study, the model was run only in forward mode (with gas + aerosol inputs) in the thermodynamically metastable phase state, assuming salts do not precipitate under supersaturated conditions. More information regarding applications of ISORROPIA-II can be found in other studies (Guo et al., 2016; Weber et al., 2016; Song et al., 2018).

## 3.    RESULTS AND DISCUSSION

### 3.1    Quality Assurance and Quality Control (QA & QC)

#### 3.1.1    Certified reference materials (CRM) – detection accuracy and repeatability

Certified reference materials for both cations and anions were investigated for quality control. CRM-C and CRM-A were analyzed three consecutive times in each lab. The detection

223 accuracy (DA) of each ion was determined as the ratio of measured concentration divided by

224 its certified concentration in percentage. The results of DA of all ions are listed in Table 2.

225 **Table 2.** Detection accuracy (%) of water-soluble inorganic ions in certified reference materials
226 measured by 10 laboratories.

| Lab NO. | $F^-$ | $Cl^-$ | $SO_4^{2-}$ | $NO_3^-$ | $Na^+$ | $NH_4^+$ | $K^+$ | $Mg^{2+}$ | $Ca^{2+}$ |
|---------|-------|--------|-------------|----------|--------|----------|-------|-----------|-----------|
| 1 | 111.8 ± 0.2 | 107.6 ± 0.1 | 108.5 ± 2.4 | 110 ± 0.5 | 98.2 ± 0.0 | 108.7 ± 0.3 | 99.4 ± 0.2 | 95.6 ± 0.3 | 99.6 ± 0.6 |
| 2 | 89.1 ± 0.4 | 95.1 ± 0.2 | 94.0 ± 1.0 | 94.5 ± 0.5 | 102.2 ± 1.0 | 135.0 ± 6.0 | 94.9 ± 4.6 | 95.9 ± 0.2 | 92.8 ± 0.5 |
| 3 | 101 ± 1.4 | 95.9 ± 0.3 | 132.4 ± 31.4 | 97.1 ± 1.0 | 91.4 ± 0.1 | 93.5 ± 0.2 | 92.4 ± 0.2 | 105.5 ± 0.3 | 98.7 ± 0.4 |
| 4 | 94.1 ± 4.0 | 90.4 ± 0.2 | 91.9 ± 1.2 | 91.7 ± 1.4 | 93.3 ± 1.7 | 112.2 ± 0.6 | 92.0 ± 2.8 | 98.9 ± 2.0 | 100.4 ± 1.1 |
| 5 | 94.0 ± 3.1 | 99.0 ± 0.0 | 92.4 ± 0.9 | 97.7 ± 0.0 | 85.9 ± 3.2 | 89.3 ± 0.5 | 92.1 ± 4.9 | 96.1 ± 0.6 | 101.7 ± 3.0 |
| 6 | 93.3 ± 0.3 | 110.8 ± 0.5 | 89.2 ± 0.1 | 91.4 ± 0.2 | 98.2 ± 1.1 | 88.4 ± 1.1 | 92.2 ± 4.9 | 102.0 ± 2.1 | 102.6 ± 1.2 |
| 7 | 89.4 ± 2.7 | 114.5 ± 21.3 | 100.8 ± 0.0 | 105.2 ± 0.2 | 97.0 ± 1.3 | 107.5 ± 0.8 | 72.1 ± 0.8 | 93.5 ± 0.4 | 91.9 ± 1.1 |
| 8 | 92.0 ± 0.0 | 96.6 ± 0.7 | 97.4 ± 1.1 | 96.2 ± 1.2 | 97.3 ± 0.0 | 93.8 ± 0.3 | 97.3 ± 0.9 | 94.0 ± 2.1 | 89.3 ± 0.6 |
| 9 | 102.6 ± 1.5 | 105.9 ± 1.0 | 101.9 ± 4.5 | 99.1 ± 3.5 | 101.2 ± 0.1 | 110.6 ± 0.2 | 103.0 ± 0.0 | 99.7 ± 0.2 | 102.2 ± 0.3 |
| 10 | 103.4 ± 1.6 | 103.5 ± 0.7 | 99.0 ± 9.3 | 114.2 ± 2.5 | 95.3 ± 4.1 | 91.0 ± 4.1 | 91.5 ± 4.7 | 94.8 ± 3.8 | 96.3 ± 2.1 |

227

228 As reported in Table 2, most ions were observed with DA in the range 90% - 110% among 10

229 laboratories. However, $SO_4^{2-}$ in Lab-3 and $NH_4^+$ in Lab-2 were overestimated, the DA of which

230 were 132.4%±31.4% and 135.0%±6.0%, respectively. The standard deviation of $SO_4^{2-}$

231 measured by Lab-3 was the largest (31.4%), followed by $Cl^-$ measured by Lab-7 (21.3%),

232 which indicated their poor repeatability. Even though $NH_4^+$ in Lab-2 was observed with high

233 value of DA, its deviation of three repeats was relatively small, which may be attributable to

234 the evaporation of ammonium in calibration standards in Lab-2; hence, the level it represented

235 was higher than its real concentration. $K^+$ in Lab-7 was underestimated, and was observed with

236 a DA of only 72.1%±0.8%. This may be due to contamination in the water blanks or the IC

237 system, as the average concentration of $K^+$ in 3 water blanks of Lab-7 was 8.0 ng/L, much

238 higher than the median value of 10 labs (3.4 ng/L).

239

240 **3.1.2 Detection limits**

241 The detection limits (DLs) in this study were calculated as:

242　　$DL = 3 \times SD_i$　　　　　　　　　　　　　　　　　　　　　　　　　　(3)

243　　where $SD_i$ is the standard deviation of the blank filters. The mean concentrations of the ions in

244　　blanks and DLs (3SD) of all ions are provided in Table 3.

245　　**Table 3.** Mean filter blank concentrations and detection limits (3SD) (ng/m$^3$) of ions measured by 10
246　　laboratories.

| Lab | F$^-$ | | Cl$^-$ | | SO$_4^{2-}$ | | NO$_3^-$ | | Na$^+$ | | NH$_4^+$ | | K$^+$ | | Mg$^{2+}$ | | Ca$^{2+}$ | |
|---|---|---|---|---|---|---|---|---|---|---|---|---|---|---|---|---|---|---|
| | mean | 3SD | mean | 3SD | mean | 3SD | mean | 3SD | mean | 3SD | mean | 3SD | mean | 3SD | mean | 3SD | mean | 3SD |
| 1 | 2.3 | 4.0 | 33.2 | 31.5 | 74.2 | 12.7 | 64.2 | 7.1 | 78.3 | 31.3 | 37.2 | 16.6 | 7.9 | 19.6. | 3.4 | 3.9. | 50.0 | 18.2. |
| 2 | 0.2 | 0.4 | 10.9 | 11.3 | 15.6 | 2.5 | 35.3 | 14.7 | 11.5 | 8.0 | 20.8 | 5.0 | 3.4 | 1.2 | 3.2 | 6.8 | 38.1 | 54.6 |
| 3 | 2.8 | 2.0 | 6.3 | 2.7 | 8.7 | 11.7 | 15.3 | 10.5 | 0.5 | 3.4 | 9.6 | 3.9 | 0.0 | 0.0 | 0.0 | 0.0 | 6.8 | 18.8 |
| 4 | 59.6 | 195.2 | 103.6 | 229.3 | 85.3 | 25.9 | 50.3 | 159.6 | 22.8 | 29.4 | 59.6 | 123.2 | 19.1 | 26.5 | 10.1 | 1.9 | 376.4 | 90.4 |
| 5 | 4.2 | 2.7 | 50.9 | 98.6 | 33.4 | 40.8 | 25.7 | 116.5 | 51.6. | 57.7. | 46.3 | 54.7 | 22.6 | 9.4 | 45.4 | 9.4 | 268.2 | 49.8 |
| 6 | n.a. | n.a. | 251.6 | 7.4 | 55.1 | 53.6 | 24.5 | 0.0 | 56.6 | 35.9 | 35.0 | 46.1 | n.a. | n.a. | n.a. | n.a. | n.a. | n.a. |
| 7 | 2.1 | 3.9 | 11.4 | 11.8 | 37.9 | 32.7 | 14.5 | 40.3 | 6.1 | 0.0 | 5.8 | 0.0 | 4.9 | 12.4 | 1.4 | 4.5 | 7.6 | 17.3 |
| 8 | n.a. | n.a. | 29.0 | 32.8 | 17.4 | 26.1 | n.a. | n.a. | 8.7 | 22.6 | n.a. | n.a. | n.a. | n.a. | n.a. | n.a. | 20.3 | 27.1 |
| 9 | n.a. | n.a. | n.a. | n.a. | 34.8 | 32.8 | 39.5 | 22.7 | 47.4 | 12.1 | 21.2 | 8.3 | 10.1 | 5.4 | 1.6 | 0.2 | 7.1 | 32.4 |
| 10 | 29.4 | 1.3 | 19.5 | 21.1 | 59.4 | 21.3 | 78.8 | 102.2 | 24.6 | 53.3 | 33.5 | 34.2 | 31.3 | 82.1 | 4.3 | 0.0 | 10.2 | 14.6 |

247　*Note: The detection limits were calculated based on large-volume sampling (total filter size: 406.5 cm$^2$; total*
248　*sampling volume: 1560 m$^3$); n.a.: not available due to no relevant peaks being identified in the chromatography.*

249    **3.2      Mass Concentrations of PM$_{2.5}$ and Inorganic Ions**

250    **3.2.1    PM$_{2.5}$ and ion concentrations**

251    The results for PM$_{2.5}$ and all inorganic ion concentrations measured by 10 labs are presented in

252    Fig. 1. During January 16$^{th}$ – 23$^{rd}$ 2019, the daily mean PM$_{2.5}$ ranged from 8.4 to 53.8 µg/m$^3$,

253    with an average of 31.4 µg/m$^3$. Among them, January 16$^{th}$, 17$^{th}$ and 18$^{th}$ were deemed

254    moderately polluted days with PM$_{2.5}$ concentration $>$ 35 µg/m$^3$, while the rest were non-haze

255    days with PM$_{2.5}$ concentrations falling in the range of 8.4-27.9 µg/m$^3$.

256
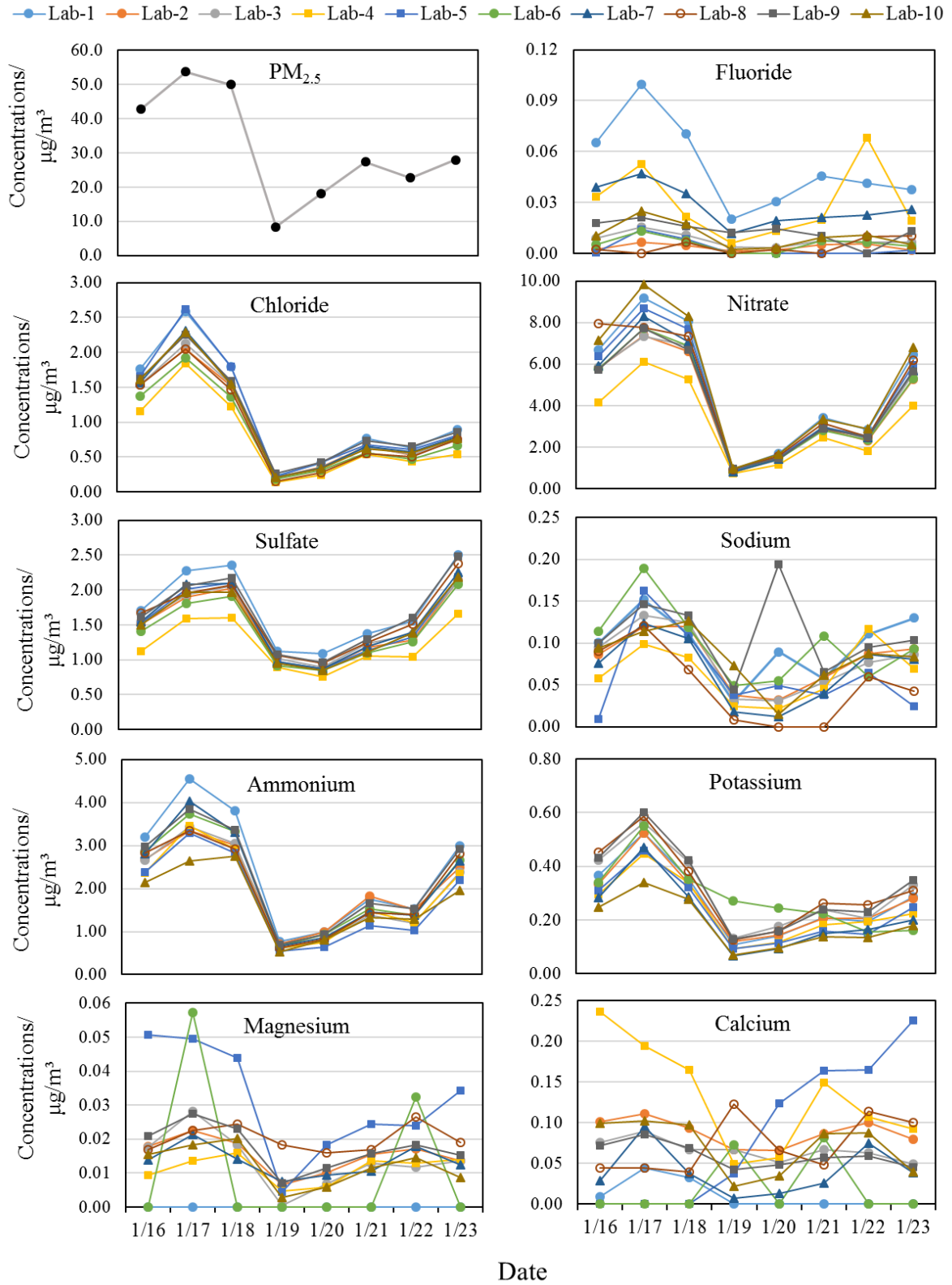
Fig. 1 The time series of mass concentrations of PM$_{2.5}$ and ions

260   The time series of all inorganic ions are also shown in Fig. 1 to demonstrate the consistency

261   among different laboratories. In Fig. 1, $Cl^-$, $NO_3^-$, $SO_4^{2-}$ and $NH_4^+$ showed a similar trend to

262   $PM_{2.5}$ and good correlations among the 10 labs, suggesting the consistency and reliability of

263   using Ion Chromatography for analysing these ions, despite various instruments and analysing

264   methods. Larger variations of $Cl^-$, $NO_3^-$, $SO_4^{2-}$ and $NH_4^+$ concentrations between different

265   laboratories were observed in moderately polluted days, whereas results for the non-haze days,

266   especially for $19^{th}$ and $20^{th}$, were observed with good agreement in 10 labs. Good agreement

267   was also observed for the mass ratios of $NO_3^-/SO_4^{2-}$ in most of the labs during the study period

268   (Fig. S4), which basically followed a similar trend as $PM_{2.5}$. On more polluted days,

269   $NO_3^-/SO_4^{2-}$ ratios were obviously higher than less polluted days, suggesting the dominance of

270   mobile source contributions over stationary sources during heavily polluted days.

271

272   The average SNA concentrations of 8 samples varied from 6.3±3.3 (Lab-4) to 9.1±5.0 (Lab-1)

273   $\mu g/m^3$ in 10 labs, accounting for 20.6±4.8 % to 29.0±6.7 % of the $PM_{2.5}$ mass concentrations.

274   However, their contributions to total ions measured by each lab were not significantly different,

275   which ranged between 83.6±2.7% and 86.3±2.3%. The total ions summed to 24.3±4.9% (Lab-

276   4) to 33.8±7.1% (Lab-1) of $PM_{2.5}$. These results are comparable with those in another study in

277   Beijing which found that SNA accounted for 88% of total ions and 9-70% of $PM_{2.5}$

278   concentrations (Xu et al., 2019b). As shown in Table 2, the DA of most ions measured by Lab-

279   4 were < 100%, while those of Lab-1 were much higher, especially for major ions (>100%).

280   Corresponding to this, the ion concentrations in Lab-4 were mostly lower than other labs, while

281   those of Lab-1 were mostly higher than other labs. For Lab-6 which was also observed to have

282   lower DA of ions such as $SO_4^{2-}$ (89.2%) and $NH_4^+$ (88.4%) in 10 labs; its SNA concentrations

283   and total ions accounted for 24.5±5.6 % and 28.7±6.0% of $PM_{2.5}$, respectively, the second

284    lowest among all labs. Hence, it is very important to run certified reference materials before

285    any sample analysis to ensure accuracy and good quality of data.

286

287    $K^+$ concentrations analysed by 10 labs followed a similar trend to $PM_{2.5}$ mass, except the

288    sample measured on a moderately polluted day ($19^{th}$) by Lab-6, which is 2-3 times higher than

289    that measured by other labs. $F^-$ concentrations varied across 10 labs, but most of them shared

290    a similar trend. Some labs like Lab-8 did not follow the same trend due to reporting

291    undetectable $F^-$ concentrations. The $Na^+$ concentration on the least polluted day ($20^{th}$) was

292    abnormally high in Lab-9, while its concentrations measured by other labs were generally low.

293    This could be due to $Na^+$ contamination during preparation or measurement of this sample, as

294    $Na^+$ concentrations in the rest of the samples measured by Lab-9 followed a similar trend as

295    that of other labs. The alkaline ions $Mg^{2+}$ and $Ca^{2+}$ are mostly originated from crustal dust and

296    mainly exist in coarse particles (Zou et al., 2018). Their mass concentrations varied

297    considerably due to their relatively low concentrations in aerosol samples and being sometimes

298    below the detection limits in some labs, such as Lab-6. Nevertheless, some labs like Lab-2, 3,

299    and 10 still followed a similar trend.

300

301    **3.2.2    Comparison with ToF-ACSM data**

302    As shown in Fig. 1, $Cl^-$, $NO_3^-$, $SO_4^{2-}$, $NH_4^+$ generally exhibited similar patterns, but due to

303    some outliers, such as $NO_3^-$ concentration measured by Lab-8 on the $16^{th}$ , the median values

304    were selected to better represent the general levels and theoretical actual concentrations of ions

305    measured by different labs. The scatter plots of the median mass concentrations of $Cl^-$, $NO_3^-$,

306    $SO_4^{2-}$ and $NH_4^+$ in 10 labs (IC- $Cl^-$, $NO_3^-$, $SO_4^{2-}$ and $NH_4^+$) *versus* the non-refractory (NR)

307    species measured by the ToF-ACSM (ACSM- $Cl^-$, $NO_3^-$, $SO_4^{2-}$ and $NH_4^+$) are shown in Fig. 2.

308    The time series of IC and ACSM data at IAP and BUCT are plotted in Fig. S5.

309    Chloride is reported to arise mainly from biomass burning and coal combustion in China

310    (Zhang et al., 2016). Its average concentration in 10 labs correlated very well with ACSM-$Cl^-$

311    ($R^2$=0.82 for IAP). However, IC-$Cl^-$ in IAP is 2-3 times higher than ACSM-$Cl^-$; this may be

312    due to the small contribution of $Cl^-$ to the overall mass spectrum which made it difficult to

313    quantify by ToF-ACSM (Allan et al., 2004). Additionally, the ACSM is incapable of measuring

314    $Cl^-$ in the form of KCl, as the ACSM only measures non-refractory $Cl^-$. Poor correlation of

315    chloride ($R^2$=0.21) was also discovered between two collocated ACSMs with a much larger set

316    of data points, while other NR species were observed with strong correlation ($R^2$>0.8) in

317    another study (Budisulistiorini et al., 2014), suggesting the quantification of chloride by ACSM

318    has large uncertainties.

319    Sulfate, as another important component of atmospheric secondary inorganic aerosols, plays

320    an important role in the formation of haze (Wang et al., 2014; Yue et al., 2019). The correlation

321    coefficient ($R^2$) between the measured IC-$SO_4^{2-}$ and ACSM-$SO_4^{2-}$ was only 0.26 for IAP with

322    a slope of 0.54. The correlation of IC-$SO_4^{2-}$ and ACSM-$SO_4^{2-}$ from BUCT was 0.84 ($R^2$) with

323    a slope of 0.56. Judging from the slopes, ACSM-$SO_4^{2-}$ and ACSM- $NH_4^+$ were similarly higher

324    than the median values of measured $SO_4^{2-}$ and $NH_4^+$ concentrations in this study. The NR

325    species followed the same trend as NR-$PM_{2.5}$, and chemical species measured through filter

326    analysis also shared the same trend as $PM_{2.5}$ measured in our study.

327    Very good correlation between measured IC and ACSM data was found for $NO_3^-$ and $NH_4^+$

328    with $R^2$>0.9. The lab median value of $NO_3^-$ was very close to the ACSM-$NO_3^-$ from the same

329    sampling site- IAP, with a slope of 0.88 for IC-$NO_3^-$/ ACSM-$NO_3^-$, while that of BUCT was

330    only 0.57. The slopes of IC-$NH_4^+$/ ACSM-$NH_4^+$ were 0.58 and 0.60 for IAP and BUCT,

331    respectively. Comparing IC-$NH_4^+$ to ACSM-$NH_4^+$, the absolute concentration of IC-$NH_4^+$

332    differed the most among all ions (42%), except $Cl^-$. Generally, ACSM-$NO_3^-$ and ACSM-$NH_4^+$

333    were higher than the median values of measured $NO_3^-$ and $NH_4^+$ concentrations in the 10 labs.

334  Higher concentrations in the online ACSM observations compared to the daily filter sample

335  measurements may be partially due to differences in the performance of the two $PM_{2.5}$ cut-

336  point selectors, which lead to different transmission efficiency of particles. Other reasons could

337  be: 1) the uncertainties in ACSM observations themselves. Crenn et al. (2015) reported the

338  uncertainties of $NO_3^-$, $SO_4^{2-}$, and $NH_4^+$ in ACSM analysis were 15%, 28%, and 36%,

339  respectively; 2) negative filter artefacts, such as volatilization of semi-volatile ions (Kim et al.,

340  2015), although that the latter would not be expected to affect sulfate. Sun et al. (2020) also

341  compared ACSM and filter based IC results and showed that the concentrations of $NO_3^-$, $NH_4^+$

342  and $SO_4^{2-}$ in the ACSM measurement were also higher than those of filter-based, although the

343  slopes were smaller than in our study. It is also possible that the representative ions of ACSM-

344  $NO_3^-$ and -$NH_4^+$ could have significant interferences from other species in the mass spectrum,

345  causing large uncertainties even after correction for those interferences.

346  To summarize, $SO_4^{2-}$, $NO_3^-$, $NH_4^+$ from lab analysis generally correlated very well with the

347  ACSM data, but the absolute concentrations differ by up to 42%. $Cl^-$ from the two methods is

348  correlated but the concentration differ by more than a factor of three. It appears that $Cl^-$ is less

349  accurate in online ACSM observations. $NO_3^-$ was comparable for the online data and filter-

350  based data, while $SO_4^{2-}$ and $NH_4^+$ in online data may be generally overestimated by a similar

351  factor. It should be noted that higher $SO_4^{2-}$ concentrations in online ACSM data could

352  potentially be due to ACSM not being able to separate organosulfate from sulfate. ACSM-$NO_3^-$,

353  -$SO_4^{2-}$ and -$NH_4^+$ were also reported to be higher (approximately 10-20%) than filter analysis

354  based $NO_3^-$, $SO_4^{2-}$ and $NH_4^+$ in another study (Sun et al., 2020).  Although the comparison

355  between IC and ACSM provided important information about the data from the two methods,

356  we recognize that we only have 8 data points here. Future studies should be carried out and

357  include more data points in order to comprehensively study the relationship between the online

358    ACSM data and filter-based data. We emphasize that it is essential that both ACSM and filter-

359    based observations are robustly quality controlled before any ACSM and IC intercomparison.

360



361
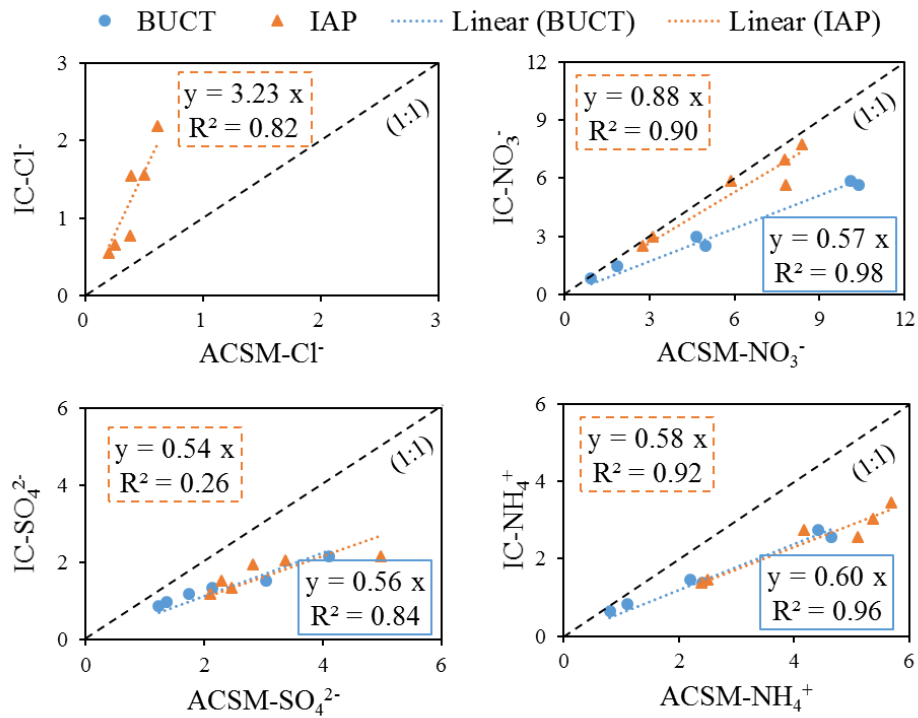
**Fig. 2** Scatter plots of the median mass concentrations of $Cl^-$, $NO_3^-$, $SO_4^{2-}$ and $NH_4^+$ measured
by 10 labs (IC- $Cl^-$, $NO_3^-$, $SO_4^{2-}$ and $NH_4^+$) *versus* the non-refractory (NR) chemical species
from ACSM (ACSM- $Cl^-$, $NO_3^-$, $SO_4^{2-}$ and $NH_4^+$) from BUCT and IAP.

365

### 3.3    Divergence and Correlation Analysis

367    As shown above, some ions like $Cl^-$, $NO_3^-$, $SO_4^{2-}$, $NH_4^+$ generally exhibited similar patterns,

368    but some of the ions varied significantly in different laboratories. Therefore, the Pearson's

369    correlation coefficient (R) and the coefficient of divergence (COD) were both calculated to

370    identify the uniformity and divergence of ionic concentrations measured by different labs. The

371    COD and R values of all ions for $Lab_j$/Lab-Median pairs are presented in Fig. 3. $Cl^-$, $NO_3^-$,

372    $SO_4^{2-}$, $NH_4^+$ and $K^+$ clearly showed high R values (>0.8) and low COD values (<0.2) in all

373    labs, suggesting the reliability of the measurement of these ions in different labs. However, $F^-$

374    and $Ca^{2+}$ in most labs was observed with higher COD values, and $Ca^{2+}$ was also found with

lower R, suggesting heterogeneity of $Ca^{2+}$ detection in different labs, which made this ion less
reliable. $Mg^{2+}$ was observed with good correlation (>0.7) between each lab and the Lab-Median,
but a higher COD was found between Lab-3, 5, 6 with the Lab-Median. Similarly, $Na^+$ was
also observed with good correlation (>0.7) between each lab and the Lab-Median, except Lab-
9, and a higher COD was found between Lab-5, 8 with the Lab-Median.
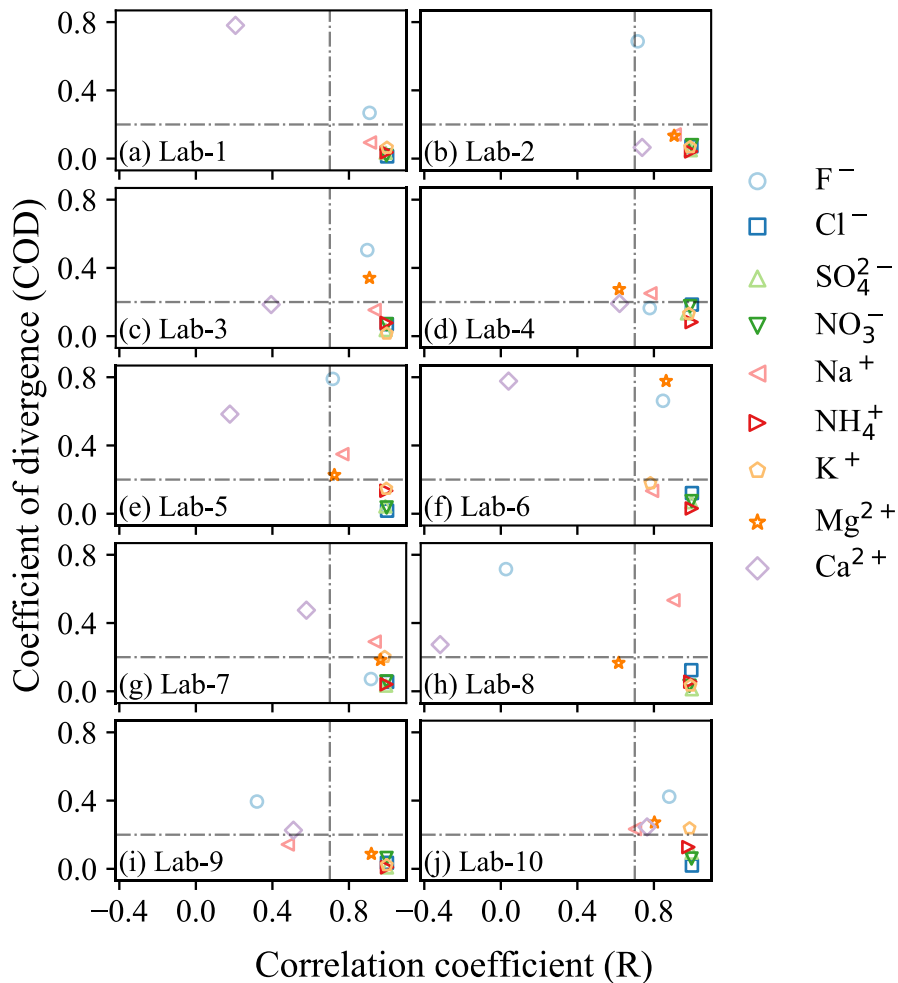


**Fig. 3** Coefficient of divergence (COD) plotted against correlation coefficient (R) for all ions
in each lab with the median ionic concentrations of 10 labs. (Note: vertical line indicates an R
value of 0.8, and horizontal lines indicate COD values of 0.2).

### 3.4 Ion Concentrations calculated by Detection Accuracy of CRM

The detection accuracy of the certified reference materials was used to correct the ion
concentrations in this study to show the importance of using CRM for calibration check and

388     quality control. The correction was conducted by dividing the measured ion concentrations by

389     their corresponding DA value. The coefficient of variation (CV) which can indicate the

390     variance of data, was applied here to compare the variation of uncorrected/corrected ion

391     concentrations among 10 labs. It was calculated as the standard deviation of ion concentrations

392     measured by 10 labs divided by the mean and expressed in a percentage. A lower CV value

393     indicates the closeness of data measured by 10 labs and reflects more precise results, while

394     higher CV value reflects the opposite. As $F^-$, $Na^+$, $Mg^{2+}$ and $Ca^{2+}$ were undetectable in some

395     labs, only $Cl^-$, $SO_4^{2-}$, $NO_3^-$, $NH_4^+$ and $K^+$ were investigated and the results are shown in Table

396     4.

397

398     In Table 4, Lab-7 was excluded from the calculation of CV of both uncorrected and corrected

399     chloride, due to its poor repeatability. The CV of uncorrected chloride concentration in 8

400     samples varied between 11.7-19.3%, with an average of 14.3%. CV of corrected chloride

401     concentration in 8 samples varied between 10.4-17.0%, with an average of 12.6%. The

402     averaged CV decreased 1.7% for corrected chloride concentration. Small changes of CV were

403     observed during moderately polluted days ($16^{th}$, $17^{th}$, $18^{th}$), but more obvious changes occurred

404     during non-haze days.

405

406     The average CV of $SO_4^{2-}$ surprisingly increased from 9.8% for uncorrected to 10.9% for

407     corrected $SO_4^{2-}$ (Supplemental Table S4). However, when excluding Lab-3 from the

408     calculation, the averaged CV of uncorrected sulfate concentration was 10.3% and it

409     significantly decreased to 6.9% once corrected. Therefore, it is strongly recommended that

410     excessive DA (>110%) with large variation should be avoided for the correction of $SO_4^{2-}$

411     concentrations. Better agreements of $NO_3^-$ and $K^+$ concentrations among 10 labs were also

observed after correction, as indicated by lower CV values for corrected samples. Similar to

other ions, the mean concentration of $NH_4^+$ of the 10 labs remained almost the same after

correction, but the CV of corrected samples increased from 12.5% to 13.2% after correction

(Table S4). Nevertheless, it decreased 1.2% after correction when excluding Lab-2 (the DA of

$NH_4^+$ was 135.0±6.0 %) from the calculation. The small change of coefficient of variation here

could be due to the high volatility of ammonia which leads to differing results measured by

different analytical procedures in labs.


To sum up, certified reference materials should be applied for the quality control. If the values

of DA are highly deviated from 100% (e.g., >110% or <90%) or there is large inter-CRM

variations, then the measurement procedures have to be checked, including repeating the

analysis or re-preparing the calibration standard solutions.


**Table 4.** Uncorrected and CRM-corrected ion concentrations ($\mu g/m^3$) and their corresponding coefficient of variations (CV/ %).

| | Uncorrected Mean (min-max) | CV/% | Corrected Mean (min-max) | CV/% | Uncorrected Mean (min-max) | CV/% | Corrected Mean (min-max) | CV/% |
|---|---|---|---|---|---|---|---|---|
| | Chloride | | | | Sulfate | | | |
| 2019/1/16 | 1.5 (1.2-1.8) | 11.7 | 1.5 (1.2-1.7) | 10.4 | 1.5 (1.1-1.7) | 11.3 | 1.6 (1.2-1.7) | 8.8 |
| 2019/1/17 | 2.2 (1.8-2.6) | 12.4 | 2.2 (1.7-2.6) | 11.3 | 2.0 (1.6-2.3) | 9.7 | 2.0 (1.7-2.2) | 6.0 |
| 2019/1/18 | 1.5 (1.2-1.8) | 11.9 | 1.5 (1.2-1.8) | 11.2 | 2.0 (1.6-2.4) | 10.2 | 2.1 (1.7-2.3) | 7.3 |
| 2019/1/19 | 0.2 (0.1-0.3) | 19.3 | 0.2 (0.2-0.2) | 16.8 | 1.0 (0.9-1.1) | 7.9 | 1.0 (1.0-1.1) | 4.5 |
| 2019/1/20 | 0.3 (0.2-0.4) | 19.0 | 0.3 (0.3-0.4) | 17.0 | 0.9 (0.8-1.1) | 10.7 | 0.9 (0.8-1.0) | 6.7 |
| 2019/1/21 | 0.6 (0.5-0.8) | 12.6 | 0.6 (0.5-0.7) | 11.0 | 1.2 (1.1-1.4) | 8.7 | 1.2 (1.1-1.3) | 4.7 |
| 2019/1/22 | 0.5 (0.4-0.7) | 13.4 | 0.5 (0.4-0.6) | 11.3 | 1.4 (1.0-1.6) | 12.5 | 1.4 (1.1-1.6) | 8.8 |
| 2019/1/23 | 0.8 (0.5-0.9) | 13.9 | 0.8 (0.6-0.8) | 12.0 | 2.2 (1.7-2.5) | 11.6 | 2.3 (1.8-2.4) | 8.5 |
| Average | | 14.3 | | 12.6 | | 10.3 | | 6.9 |
| | Nitrate | | | | Ammonium | | | |
| 2019/1/16 | 6.1 (4.1-8.0) | 16.5 | 6.1 (4.5-8.3) | 15.2 | 2.7 (2.1-3.2) | 12.7 | 2.7 (2.1-3.2) | 12.8 |
| 2019/1/17 | 8.0 (6.1-9.8) | 13.1 | 8.0 (6.7-8.9) | 7.8 | 3.6 (2.6-4.5) | 14.9 | 3.6 (2.9-4.2) | 12.1 |
| 2019/1/18 | 7.1 (5.3-8.3) | 12.1 | 7.1 (5.7-7.9) | 8.4 | 3.1 (2.7-3.8) | 10.8 | 3.2 (2.6-3.8) | 10.2 |
| 2019/1/19 | 0.9 (0.7-0.9) | 8.9 | 0.9 (0.8-1.0) | 7.3 | 0.6 (0.5-0.8) | 11.7 | 0.6 (0.6-0.7) | 9.4 |
| 2019/1/20 | 1.5 (1.2-1.7) | 9.8 | 1.5 (1.3-1.6) | 7.0 | 0.8 (0.6-1.0) | 13.1 | 0.8 (0.7-1.1) | 13.3 |
| 2019/1/21 | 3.0 (2.4-3.4) | 9.4 | 3.0 (2.7-3.3) | 5.9 | 1.5 (1.1-1.7) | 12.1 | 1.5 (1.3-1.7) | 9.7 |

| | | | | | | | | |
|---|---|---|---|---|---|---|---|---|
| 2019/1/22 | 2.4 (1.8-2.9) | 12.3 | 2.5 (2.0-2.6) | 7.9 | 1.3 (1.0-1.5) | 12.3 | 1.3 (1.1-1.6) | 11.8 |
| 2019/1/23 | 5.7 (4.0-6.8) | 13.6 | 5.7 (4.4-6.4) | 9.6 | 2.5 (2.0-3.0) | 13.7 | 2.6 (2.1-3.0) | 12.6 |
| Average | | 12.0 | | 8.6 | | 12.7 | | 11.5 |
| | Potassium | | | | | | | |
| 2019/1/16 | 0.3 (0.2-0.5) | 19.8 | 0.4 (0.3-0.5) | 16.2 | | | | |
| 2019/1/17 | 0.5 (0.3-0.6) | 15.6 | 0.5 (0.4-0.7) | 14.9 | | | | |
| 2019/1/18 | 0.3 (0.3-0.4) | 14.1 | 0.4 (0.3-0.5) | 10.8 | | | | |
| 2019/1/19 | 0.1 (0.1-0.3) | 48.5 | 0.1 (0.1-0.3) | 47.7 | | | | |
| 2019/1/20 | 0.1 (0.1-0.2) | 31.4 | 0.2 (0.1-0.3) | 29.7 | | | | |
| 2019/1/21 | 0.2 (0.1-0.3) | 20.9 | 0.2 (0.2-0.3) | 17.0 | | | | |
| 2019/1/22 | 0.2 (0.1-0.3) | 20.6 | 0.2 (0.1-0.3) | 17.8 | | | | |
| 2019/1/23 | 0.3 (0.2-0.3) | 25.3 | 0.3 (0.2-0.4) | 21.3 | | | | |
| Average | | 24.5 | | 21.9 | | | | |

*Lab-2, 3 and 7 were excluded for calculating CV% of ammonium, sulfate and chloride, respectively.*

## 3.5    Aerosol Acidity

In this study, aerosol acidity was evaluated applying three different parameters: Anion and Cation Equivalence Ratio, ion-balance and in situ acidity. Ion-balance was calculated by subtracting equivalent cations from anions (Zhang et al., 2007), while in-situ aerosol acidity was represented by pH or the concentration of free $H^+$ in the deliquesced particles under ambient conditions. In situ aerosol pH can be estimated from various thermodynamic models, for example, SCAPE, GFEMN, E-AIM and ISORROPIA (He et al., 2012; Pathak et al., 2009; Yao et al., 2006). In situ aerosol acidity is most likely to influence the chemical behavior of aerosols (He et al., 2012). Ion-balance is widely used to indicate the neutralization status of aerosols with the equivalent ratios of anions/cations in a relative way (Sun et al., 2010; Takami et al., 2007; Chou et al., 2008). It is noteworthy that ion-balance and in-situ aerosol acidity estimations are empirical approaches which are strongly dependent on the selection of ion species.

### 3.5.1 Anion and Cation Equivalence Ratio

The ratio of the anion molar equivalent concentrations to the cation molar equivalent concentrations (AE/CE) can be applied to reflect the potential aerosol acidity (Meng et al., 2016; Zou et al., 2018). In this study, AE and CE were calculated as:

$$AE = [SO_4^{2-}/96] \times 2 + [NO_3^-/62] + [Cl^-/35.5] + [F^-/19] \qquad (4)$$

$$CE = [NH_4^+/18] + [Na^+/23] + [K^+/39] + [Mg^{2+}/24] \times 2 + [Ca^{2+}/40] \times 2 \qquad (5)$$

AE represents the equivalent concentrations of all anions; and CE denotes all cations equivalent concentrations.

**Table 5.** Anion and cation equivalent ratios (AE/CE) among 10 laboratories.

|  | Lab-1 | Lab-2 | Lab-3 | Lab-4 | Lab-5 | Lab-6 | Lab-7 | Lab-8 | Lab-9 | Lab-10 |
|---|---|---|---|---|---|---|---|---|---|---|
| 2019/1/16 | 1.02 | 1.01 | 1.02 | 0.81 | 1.26 | 0.93 | 1.03 | 1.18 | 0.93 | 1.43 |
| 2019/1/17 | 1.00 | 1.02 | 1.01 | 0.85 | 1.25 | 0.93 | 0.87 | 1.07 | 0.96 | 1.59 |
| 2019/1/18 | 1.03 | 1.03 | 1.04 | 0.84 | 1.26 | 0.96 | 1.03 | 1.14 | 0.95 | 1.28 |
| 2019/1/19 | 0.99 | 0.79 | 0.97 | 0.85 | 1.11 | 0.65 | 0.99 | 0.90 | 0.98 | 1.15 |
| 2019/1/20 | 1.00 | 0.80 | 0.96 | 0.85 | 1.14 | 0.82 | 1.00 | 0.98 | 0.83 | 1.08 |
| 2019/1/21 | 1.03 | 0.78 | 1.03 | 0.80 | 1.14 | 0.85 | 1.04 | 1.02 | 0.90 | 1.12 |
| 2019/1/22 | 1.04 | 0.79 | 1.04 | 0.80 | 1.16 | 0.90 | 0.97 | 0.91 | 0.93 | 1.09 |
| 2019/1/23 | 1.02 | 0.98 | 1.05 | 0.80 | 1.15 | 0.95 | 0.84 | 1.00 | 0.94 | 1.48 |

As presented in Table 5, the AE/CE ratio of all samples were compared among 10 labs. The ratios in Lab-1 and Lab-3 were close to unity. The ratios in Lab-5 and Lab-10 were above 1, indicating the deficiency of cations to neutralize all anions, while that was the contrary of Lab-4, 6 and 9. In Table 2, the detection accuracies of major cations ($Na^+$, $NH_4^+$, $K^+$) were <100% and much lower than those of the major anions ($Cl^-$, $NO_3^-$, $SO_4^{2-}$) in Lab-5 and 10, which may have caused lower cation concentrations than their real concentrations and a constant higher ratio of AE/CE. For Lab-9, the detection accuracies of all ions were very close to 100%, except

24

462  $NH_4^+$ which was found with a detection accuracy of >110%. Therefore, AE/CE < 1 of all

463  samples measured by Lab-9 could be the result of overestimation of ammonium. Similarly, in

464  addition to ammonium detection accuracy of >110%, generally lower anion detection

465  accuracies than cations were reported by Lab-4, which may explain AE/CE < 1 in all samples

466  measured by this lab as well. The other three labs (Lab-2, 7 and 8) were found with various

467  AE/CE ratios with both >1 and <1 values; moderately polluted days were generally observed

468  with a higher ratio of AE/CE. These results indicate that AE/CE ratios bear large uncertainties

469  from different labs. Stricter quality control measures should be adopted if applying AE/CE

470  ratios to evaluate aerosol acidity.

471

472  **3.5.2    Ion Balance**

473  The calculation of ion balance is an alternative way to evaluate the aerosol acidity (Han et al.,

474  2016; He et al., 2012). Three methods were listed below for the calculation of ion balance in

475  this study:

476  Method 1: $IB = 2[SO_4^{2-}] + [NO_3^-] - [NH_4^+]$ (6)

477  Method 2: $IB = 2[SO_4^{2-}] + [NO_3^-] + [Cl^-] - [NH_4^+] - [Na^+] - [K^+]$ (7)

478  Method3:   $IB = 2[SO_4^{2-}] + [NO_3^-] + [Cl^-] - [NH_4^+] - [Na^+] - [K^+] - 2[Mg^{2+}] - 2[Ca^{2+}]$

479                                                                                                (8)

480  In Method 1, only $SO_4^{2-}$, $NO_3^-$ and $NH_4^+$ were applied for the calculation (Tian et al., 2017),

481  assuming that these three ions and $H^+$ alone control $PM_{2.5}$ acidity (Ziemba et al., 2007). $SO_4^{2-}$,

482  $NO_3^-$ and $NH_4^+$ were also used in other studies to assess aerosol acidity. For example, the mole

483  charge ratio of $NH_4^+$ to the sum of $SO_4^{2-}$ and $NO_3^-$ was applied to represent aerosol acidity

484  (Chandra Mouli et al., 2003; Wang et al., 2019). $SO_4^{2-}$, $NO_3^-$ and $NH_4^+$ were selected because

485  they contributed approximately 90% of the total ionic species in fine aerosols and play

486    predominant roles in controlling aerosol acidity (Zhou et al., 2012). Salt ions $Na^+$, $K^+$ and $Cl^-$

487    were added for the calculation in Method 2. Based on this calculation, $Mg^{2+}$ and $Ca^{2+}$ were

488    added in Method 3 to include the effects of crustal dust on aerosol acidity (Huang et al., 2014).

489    The ion balance of all labs varied applying different methods, especially for the first three

490    heavily polluted days, as shown in Fig. 4. Positive ion balance values indicated a deficiency of

491    cations to neutralize anions, while negative values implied an excess of cations to neutralize

492    anions. Lab-10 showed the highest variation among all labs; when excluding Lab-10, the results

493    of the other 9 labs agreed very well, with most of the values below 0, suggesting sufficient

494    ammonium to neutralize sulfate and nitrate. By applying Method 1, comparable results were

495    found. The average ion balance values in all samples were consistent in Lab-1, 2, 6, 7, 9 (0.02

496    $\mu mol/m^3$). When adding more ions in the calculation by adopting Methods 2 and 3, poorer

497    agreement among all labs was exhibited. Therefore, it seems more consistent to indicate the

498    relative ion-balanced aerosol acidity among different samples by Method 1, as SNA were the

499    most abundant ions in atmospheric aerosols and their concentrations measured by different labs

500    showed good agreement (Fig. 1). This method could reduce the large discrepancy of ion

501    balance results calculated by adding other ions from the different labs, as their concentrations

502    varied largely in different labs due to varying detection limits.

503
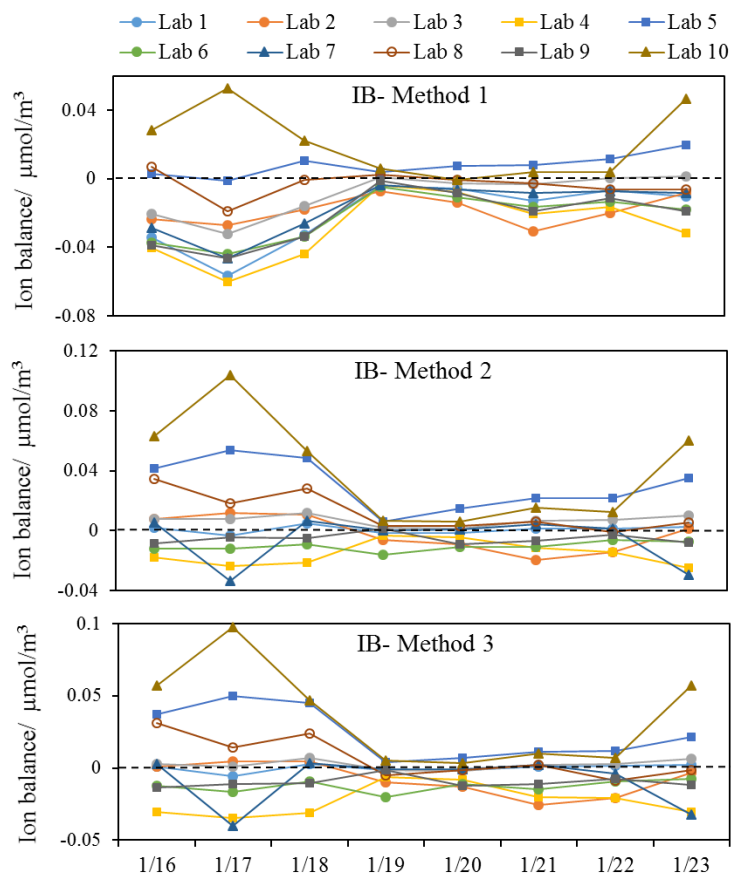
**Fig. 4** Ion balance in all labs applying different methods (negative values reflect the excessive cations to neutralize anions)

### 3.5.3 Aerosol pH using ISORROPIA-II

A thermodynamic equilibrium model- ISORROPIA-II was applied to estimate the in-situ aerosol acidity. This was run only in forward mode, as the results from the use of reverse mode (using only particle phase composition) are reported to be unreliable (Song et al., 2018) . The only gas phase data were for ammonia, but this introduces little error as concentrations of $HNO_3$ and HCl are likely to be very low in this high ammonia environment (Song et al., 2018) .

The inputs include aerosol-phase $Cl^-$, $SO_4^{2-}$, $NO_3^-$, $Na^+$, $NH_4^+$, $K^+$, $Mg^{2+}$, $Ca^{2+}$ and gas-phase $NH_3$ concentrations. The daily ammonia concentrations during the study period derived from 5-minute data ranged from 13.9±0.6 to 20.1±0.7 ppb (average: 17.2±2.2 ppb). The small standard deviations of the daily average (< 1 ppb) suggest that the diurnal variation of $NH_3$ was not significant. Hence, aerosol pH was only investigated using daily mean $NH_3$ concentrations.

27

519    Mean $NH_3$ concentrations during moderately polluted and non-haze days were 19.6±0.6 and

520    15.9±1.5 ppb, respectively. Daily temperature ranged between -4.4°C to 4.3°C with an average

521    of 1.0°C and RH ranged from 13.8% to 40.1% with a mean value of 22.4%. The aerosol pH

522    was calculated for all samples by the model, as well as aerosol water content (AWC. Table S5),

523    details of the calculation of pH and AWC can be found elsewhere (Liu et al., 2017b; Masiol et

524    al., 2020). The calculated aerosol pH results of 10 labs are presented in Fig. 5. The predicted

525    gas-phase $NH_3$ by ISORROPIA-II was well correlated with the measured $NH_3$ with slope of

526    1.02 and $R^2$ of 0.95 (Fig. S6), which demonstrated the accuracy of thermodynamic calculations

527    by the model (Song et al., 2018).
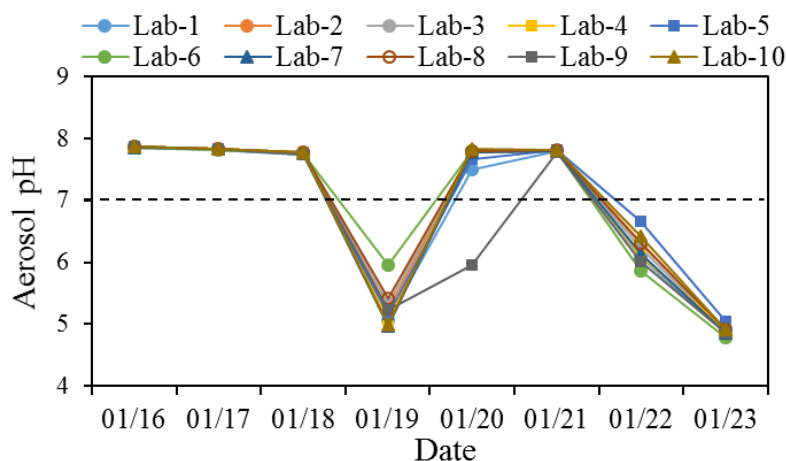


528
529    **Fig. 5** Aerosol pH estimated by ISORROPIA-II using ions and ammonia in 10 labs from 16th to 23rd
530    January 2019.

531

532    The computed aerosol pH during the study period generally exhibited good agreement among

533    10 labs. Lab-6 was observed with higher pH and lower ion balance than other labs on the 19th,

534    which could be mainly due to the 2-3 times higher $K^+$ concentration measured by Lab-6 on that

535    day (Fig. 1), while other ions measured by this lab were more comparable with other labs. The

536    aerosol pH on 3 moderately polluted days was above 7, indicating an alkaline nature of aerosols

537    during these days. This result is consistent with the discussion mentioned above that ion

538    balance estimated by Method 1 was below 0 as more $NH_4^+$ neutralizes $NO_3^-$ and $SO_4^{2-}$. It should

be noted that higher pH (>7) of those samples could be due to the lower temperature (-4.4~4.3 °C) during the sampling period (Table S3), in addition to their relatively alkalic nature. The equilibrium of water ($H_2O$) with $OH^-$(aq) + $H^+$(aq) is temperature-dependent. For highly dilute aqueous systems, the values of $pK_w$ (= $-\log_{10}[K_w]$; $K_w$ is the temperature-dependent equilibrium constant on molality basis) at 25 °C (13.99) and 0 °C (14.95) can result in corresponding pH values of 6.995 and 7.475, respectively, both of which are considered neutral (Bandura and Lvova, 2006; Pye et al., 2020). In addition, the low RH in these samples (Table S3) may have also contributed to the high pH values we calculated. Different RH values were tested for aerosol pH among 10 labs. The results (Fig. S7) showed that at different RH (40%, 50%, 60%, 70%, 80%), the pH values in 10 labs were consistent; and the pH values were mostly lower than 6 in all samples. Hence, higher pH (>7) of some samples could be resulted from the combination of lower temperature, RH, and the nature of the aerosols. Excellent agreement among the 10 labs for the aerosol pH during these moderately polluted days was also found. Non-haze days, especially the least polluted day on 20th, showed higher variation among the different labs. The calculated pH of 9 labs mostly fall on the same side of the neutralization line (pH=7), and only lab-9 on 20th falls onto a different side of the pH=7 line from the other labs. Sensitivity test of $Na^+$, $K^+$, $Mg^{2+}$ and $Ca^{2+}$ showed that this abnormal pH value was mainly due to the significant higher $Na^+$ concentration of Lab-9 on 20th.

Our results suggest AE/CE and Ion Balance are flawed representations of particle acidity, which are not recommended for the evaluation of aerosol acidity. This is also consistent with the conclusions from previous studies (Hennigan et al., 2015; Guo et al., 2015; Pye et al., 2020). ISORROPIA-II gives more consistent aerosol pH values among different laboratories. But there are uncertainties within this calculation: 1) RH during some periods in this study was relatively low (around 20%), and as a result, aerosol water content is very low. Under such conditions, ions are mostly existed in solid phase. Hence, pH of aerosols with very low RH

564 may not be reliable; 2) the calculation of AWC only considered for inorganics in this study.

565 Water associated with organics also contribute to AWC. For example, Guo et al. (2015)

566 indicated that it accounts for 29-39% of total $PM_{2.5}$ water in southeastern United States.

567 $NH_3$ is the main driving factor affecting aerosol pH and leads to the more alkaline nature of

568 aerosols. To investigate the effect of $NH_3$ concentration on aerosol pH, we conducted a

569 sensitivity test which showed the aerosol pH of samples measured by 10 labs at $NH_3$ levels of

570 0.5, 1, 2, 5 and 10 ppb (Fig. S8). When the concentration of $NH_3 \geq 2$ ppb, the aerosol pH

571 estimates of the 10 labs were generally consistent and less affected by the variation of ion

572 concentrations. But there is more variation of aerosol pH in the 10 labs when $NH_3$ concentration

573 was under 2 ppb. This suggests when $NH_3$ concentration $< 2$ ppb, the aerosol pH could be more

574 affected by the variation of ion concentrations. Wang et. al (2020) also reported that the high

575 concentration of total ammonium (gas+aerosol) was likely an important factor causing lower

576 aerosol acidity of fine particles during a severe haze period in Henan province, China. It is also

577 confirmed in another study that ammonia played an important role in influencing aerosol pH

578 during winter haze period in northern China (Song et al., 2018).

579

## 4.    SUMMARY AND RECOMMENDATIONS

581 Despite use of variable methods and instruments for measuring ion concentrations, data from

582 all the participating labs show a reasonably good agreement in the overall trend for major ions

583 like chloride, sulfate, nitrate, and ammonium. The coefficients of divergence of these ions

584 across 10 labs were lower than 0.2 and the correlation coefficients were higher than 0.8,

585 suggesting a reasonably high reliability of measuring major ions by IC in different labs.

586 However, the inter-lab difference can be as high as 30% if excluding the two extreme values

587 for each day, and reached up to 100% in extreme cases if including all data. Furthermore, ions

588    like $F^-$, $Mg^{2+}$, $K^+$ and $Ca^{2+}$ were observed with large variations in different labs, which may be

589    due to their relatively low concentrations in the samples. Good correlations were found for

590    non-refractory ion species measured by ACSM with those in our study. However, the absolute

591    mass levels were quite different, which may be due to the differences in the performance of the

592    two $PM_{2.5}$ cut-point selectors, the uncertainties in ACSM observations themselves, and

593    negative filter artefacts. Certified reference materials were applied to show the detection

594    accuracy of IC measurement in the 10 laboratories. By comparing the coefficient of variation

595    of samples among 10 labs before and after correction by the detection accuracy of CRM, we

596    emphasize the importance of using certified reference materials for quality control for future

597    ionic species analysis.

598

599    Aerosol acidity was studied through the investigation of ion-balance based acidity and in-situ

600    acidity. Firstly, the ratios of anion equivalent concentrations to cation equivalent concentrations

601    (AE/CE) varied significantly in different labs, which could be attributed to measurement errors,

602    as supported by the different detection accuracies of ions in CRM. Secondly, by calculating the

603    ion balance, Method 1 which only applied SNA for the calculation, was more consistent in

604    most labs. Poor agreement of acidity estimation was observed in all labs when adding other

605    ions like $Ca^{2+}$ and $Mg^{2+}$. Finally, ISORROPIA-II was applied for estimating in-situ aerosol

606    acidity by calculating aerosol pH in forward (gas+aerosol phases as input) mode. The results

607    showed a similar trend between labs and exhibited a good agreement. This indicates that, if

608    including gaseous pollutant equilibrium in the ISORPIA II model, the estimated aerosol pH is

609    more consistent even if there are relatively large differences in the measured concentrations of

610    ions.

611

31

Based on this analysis and our experience, we recommend that:

1.  Literature aerosol ion data based on online and offline methods should be treated with a degree of uncertainty in mind. The uncertainties are particularly large for minor ions like $Ca^{2+}$ from the aerosol filters-based ion chromatography analysis.

2.  The ion-balance approach is not recommended for estimating aerosol acidity due to its large uncertainty. Instead, in situ aerosol pH may be used to represent acidity, and can be calculated from thermodynamic model considering gas-aerosol equilibrium (e.g., $NH_4^+$ and $NH_3$). This requires the measurements of aerosol composition as well as $NH_3$.

3.  The variation of ion concentrations is expected to strongly affect aerosol acidity estimated by ISORROPIA II when the $NH_3$ concentration is low (e.g., < 2 ppb in this case). Additionally, the impact of the diurnal variation of $NH_3$ on aerosol acidity is worthy of investigation, particularly when the $NH_3$ concentration is low.

4.  Certified reference materials should be used on a regular basis to assess the accuracy and reliability of the measurement method. Calibration standards should be re-prepared and the IC performance should be checked when the detection accuracy is largely deviated from 100% (e.g., > 110% or < 90%).

5.  The detection accuracy of ammonium varied significantly among 10 labs (88.4-135.0%) with median value close to 100%. Stock $NH_4^+$ solutions that are used for the preparation of calibration standards should be freshly prepared to ensure good detection accuracy.

6.  Robust quality control processes should be put in place to avoid contamination, particularly for those ions with low concentrations, such as $K^+$ and $Na^+$. For example, water blanks should be run before any standard or sample analyses to ensure no contamination from water blanks or the IC system.

635    7.  Some batches of commercial quartz filters may be contaminated with $Na^+$ and $PO_4^{3-}$, and

636       thus testing each batch of blank filters is necessary before any field sampling (data not

637       shown here). Filter washing may be needed in some cases.

638    8.  Ionic concentration from ACSM observations should be calibrated although the observed

639       trend is robust. Future research should be carried out to compare the offline ASCM and IC

640       using the same filters to clearly identify the discrepancies between the two methods.

641

642 **ACKNOWLEDGEMENTS**

647

648 *Data availability.* The data in this article are available from the corresponding author upon
649 request.

650

651 *Author contributions.* ZS conceived the study after discovering large inter-lab variability in
652 water-soluble inorganic ions from offline and online methods. JX prepared the paper with the
653 help of ZS, RMH and all co-authors. JX, LW, QZ, CZ, XY, DC, WJL, MW, HT, LiL, ST,
654 WRL, JW, GS, YH, SS, CP, YC, FY, AM, DD, SJS, IA, and JFH conducted the laboratory
655 analysis. SS supported the aerosol pH calculation. CS supported the calculation of coefficient
656 of divergence. YLS, LuL, FZ, KRD, CY, YL, MK provided the ACSM data and YLS supported
657 the interpretation of the ACSM data. BG provided the $NH_3$ data.

658

659 *Competing interests.* The authors declare that they have no conflict of interest.

660

661 **REFERENCES**

662 Allan, J. D., Delia, A. E., Coe, H., Bower, K. N., Alfarra, M. R., Jimenez, J. L., Middlebrook, A. M.,
663 Drewnick, F., Onasch, T. B., Canagaratna, M. R., Jayne, J. T., and Worsnop, D. R.: A generalised
664 method for the extraction of chemically resolved mass spectra from Aerodyne aerosol mass

spectrometer data, Journal of Aerosol Science, 35, 909-922, https://doi.org/10.1016/j.jaerosci.2004.02.007, 2004.

Baltensperger, U., and Hertz, J.: Determination of anions and cations in atmospheric aerosols by single column ion chromatography, Journal of Chromatography A, 324, 153-161, https://doi.org/10.1016/S0021-9673(01)81314-5, 1985.

Bandura, A., and Lvova, S.: The Ionization Constant of Water over Wide Ranges of Temperature and Density, Journal of Physical and Chemical Reference Data - J PHYS CHEM REF DATA, 35, 10.1063/1.1928231, 2006.

Buchberger, W. W.: Detection techniques in ion chromatography of inorganic ions, TrAC Trends in Analytical Chemistry, 20, 296-303, https://doi.org/10.1016/S0165-9936(01)00068-1, 2001.

Budisulistiorini, S. H., Canagaratna, M. R., Croteau, P. L., Baumann, K., Edgerton, E. S., Kollman, M. S., Ng, N. L., Verma, V., Shaw, S. L., Knipping, E. M., Worsnop, D. R., Jayne, J. T., Weber, R. J., and Surratt, J. D.: Intercomparison of an Aerosol Chemical Speciation Monitor (ACSM) with ambient fine aerosol measurements in downtown Atlanta, Georgia, Atmos. Meas. Tech., 7, 1929-1941, 10.5194/amt-7-1929-2014, 2014.

Chandra Mouli, P., Venkata Mohan, S., and Jayarama Reddy, S.: A study on major inorganic ion composition of atmospheric aerosols at Tirupati, Journal of Hazardous Materials, 96, 217-228, https://doi.org/10.1016/S0304-3894(02)00214-5, 2003.

Chou, C. C. K., Lee, C. T., Yuan, C. S., Hsu, W. C., Lin, C. Y., Hsu, S. C., and Liu, S. C.: Implications of the chemical transformation of Asian outflow aerosols for the long-range transport of inorganic nitrogen species, Atmospheric Environment, 42, 7508-7519, https://doi.org/10.1016/j.atmosenv.2008.05.049, 2008.

Crenn, V., Sciare, J., Croteau, P. L., Verlhac, S., Fröhlich, R., Belis, C. A., Aas, W., Äijälä, M., Alastuey, A., Artiñano, B., Baisnée, D., Bonnaire, N., Bressi, M., Canagaratna, M., Canonaco, F., Carbone, C., Cavalli, F., Coz, E., Cubison, M. J., Esser-Gietl, J. K., Green, D. C., Gros, V., Heikkinen, L., Herrmann, H., Lunder, C., Minguillón, M. C., Močnik, G., O'Dowd, C. D., Ovadnevaite, J., Petit, J. E., Petralia, E., Poulain, L., Priestman, M., Riffault, V., Ripoll, A., Sarda-Estève, R., Slowik, J. G., Setyan, A., Wiedensohler, A., Baltensperger, U., Prévôt, A. S. H., Jayne, J. T., and Favez, O.: ACTRIS ACSM intercomparison – Part 1: Reproducibility of concentration and fragment results from 13 individual Quadrupole Aerosol Chemical Speciation Monitors (Q-ACSM) and consistency with co-located instruments, Atmos. Meas. Tech., 8, 5063-5087, 10.5194/amt-8-5063-2015, 2015.

Đorđević, D., Mihajlidi-Zelić, A., Relić, D., Ignjatović, L., Huremović, J., Stortini, A. M., and Gambaro, A.: Size-segregated mass concentration and water soluble inorganic ions in an urban aerosol of the Central Balkans (Belgrade), Atmospheric Environment, 46, 309-317, https://doi.org/10.1016/j.atmosenv.2011.09.057, 2012.

Fan, M.-Y., Cao, F., Zhang, Y.-Y., Bao, M.-Y., Liu, X.-Y., Zhang, W.-Q., Gao, S., and Zhang, Y.-L.: Characteristics and Sources of Water Soluble Inorganic Ions in Fine Particulate Matter During Winter in Xuzhou (In Chinese), Huan jing ke xue= Huanjing kexue, 38, 4478-4485, 10.13227/j.hjkx.201703178, 2017.

Fountoukis, C., and Nenes, A.: ISORROPIA II: a computationally efficient thermodynamic equilibrium model for K+–Ca2+–Mg2+–NH4+–Na+–SO42-–NO3-–Cl-–H2O aerosols, Atmos. Chem. Phys., 7, 4639-4659, 10.5194/acp-7-4639-2007, 2007.

Ge, B. Z., Xu, X. B., Ma, Z. Q., Pan, X. L., Wang, Z., Lin, W. L., Ouyang, B., Xu, D. H., Lee, J., Zheng, M., Ji, D. S., Sun, Y. L., Dong, H. B., Squires, F. A., Fu, P. Q., and Wang, Z. F.: Role of Ammonia on the Feedback Between AWC and Inorganic Aerosol Formation During Heavy Pollution in the North China Plain, Earth And Space Science, 6, 1675-1693, 10.1029/2019ea000799, 2019.

Guo, H., Xu, L., Bougiatioti, A., Cerully, K., Capps, S., Hite, J., Carlton, A. M., Lee, S.-H., Bergin, M., Ng, N., Nenes, A., and Weber, R.: Fine-particle water and pH in the southeastern United States, ATMOSPHERIC CHEMISTRY AND PHYSICS, 15, 5211-5228, 10.5194/acp-15-5211-2015, 2015.

Guo, H., Sullivan, A. P., Campuzano-Jost, P., Schroder, J. C., Lopez-Hilfiker, F. D., Dibb, J. E., Jimenez, J. L., Thornton, J. A., Brown, S. S., Nenes, A., and Weber, R. J.: Fine particle pH and the partitioning of nitric acid during winter in the northeastern United States, Journal of Geophysical Research: Atmospheres, 121, 10,355-310,376, 10.1002/2016jd025311, 2016.

718  Guo, Y.-t., Zhang, J., Wang, S.-g., She, F., and Li, X.: Long-term characterization of major water-
719  soluble inorganic ions in PM10 in coastal site on the Japan Sea, Journal of Atmospheric Chemistry, 68,
720  299-316, 10.1007/s10874-012-9223-8, 2011.
721  Han, B., Zhang, R., Yang, W., Bai, Z., Ma, Z., and Zhang, W.: Heavy haze episodes in Beijing during
722  January 2013: Inorganic ion chemistry and source analysis using highly time-resolved measurements
723  from an urban site, Science of the Total Environment, 544, 319-329, 10.1016/j.scitotenv.2015.10.053,
724  2016.
725  Harrison, R. M., and Pio, C. A.: MAJOR ION COMPOSITION AND CHEMICAL ASSOCIATIONS
726  OF  INORGANIC  ATMOSPHERIC  AEROSOLS,  Environ.  Sci.  Technol.,  17,  169-174,
727  10.1021/es00109a009, 1983.
728  He, K., Zhao, Q., Ma, Y., Duan, F., Yang, F., Shi, Z., and Chen, G.: Spatial and seasonal variability of
729  PM2.5 acidity at two Chinese megacities: insights into the formation of secondary inorganic aerosols,
730  Atmos. Chem. Phys., 12, 1377-1395, 10.5194/acp-12-1377-2012, 2012.
731  He, Q., Yan, Y., Guo, L., Zhang, Y., Zhang, G., and Wang, X.: Characterization and source analysis of
732  water-soluble inorganic ionic species in PM2.5 in Taiyuan city, China, Atmos. Res., 184, 48-55,
733  https://doi.org/10.1016/j.atmosres.2016.10.008, 2017.
734  Heckenberg, A. L., and Haddad, P. R.: Determination of inorganic anions at parts per billion levels
735  using single-column ion chromatography without sample preconcentration, Journal of Chromatography
736  A, 299, 301-305, https://doi.org/10.1016/S0021-9673(01)97845-8, 1984.
737  Hennigan, C. J., Izumi, J., Sullivan, A. P., Weber, R. J., and Nenes, A.: A critical evaluation of proxy
738  methods used to estimate the acidity of atmospheric particles, Atmos. Chem. Phys., 15, 2775-2790,
739  10.5194/acp-15-2775-2015, 2015.
740  Huang, K., Zhuang, G., Wang, Q., Fu, J. S., Lin, Y., Liu, T., Han, L., and Deng, C.: Extreme haze
741  pollution in Beijing during January 2013: chemical characteristics, formation mechanism and role of
742  fog processing, Atmos. Chem. Phys. Discuss., 2014, 7517-7556, 10.5194/acpd-14-7517-2014, 2014.
743  Jia, S., Wang, X., Zhang, Q., Sarkar, S., Wu, L., Huang, M., Zhang, J., and Yang, L.: Technical note:
744  Comparison and interconversion of pH based on different standard states for aerosol acidity
745  characterization, Atmospheric Chemistry and Physics, 18, 11125-11133, 10.5194/acp-18-11125-2018,
746  2018.
747  Kamal, A., Syed, J. H., Li, J., Zhang, G., Mahmood, A., and Malik, R. N.: Profile of Atmospheric PAHs
748  in Rawalpindi, Lahore and Gujranwala Districts of Punjab Province (Pakistan), Aerosol Air Qual. Res.,
749  16, 1010-1021, 10.4209/aaqr.2015.01.0016, 2016.
750  Karthikeyan, S., and Balasubramanian, R.: Determination of water-soluble inorganic and organic
751  species  in  atmospheric  fine  particulate  matter,  Microchemical  Journal,  82,  49-55,
752  https://doi.org/10.1016/j.microc.2005.07.003, 2006.
753  Kim, C. H., Choi, Y., and Ghim, Y. S.: Characterization of Volatilization of Filter-Sampled PM2.5
754  Semi-Volatile Inorganic Ions Using a Backup Filter and Denuders, Aerosol Air Qual. Res., 15, 814-
755  820, 10.4209/aaqr.2014.09.0213, 2015.
756  Krudysz, M. A., Froines, J. R., Fine, P. M., and Sioutas, C.: Intra-community spatial variation of size-
757  fractionated PM mass, OC, EC, and trace elements in the Long Beach, CA area, Atmospheric
758  Environment, 42, 5374-5389, https://doi.org/10.1016/j.atmosenv.2008.02.060, 2008.
759  Li, L., Yin, Y., Kong, S., Wen, B., Chen, K., Yuan, L., and Li, Q.: Altitudinal effect to the size
760  distribution of water soluble inorganic ions in PM at Huangshan, China, Atmospheric Environment, 98,
761  242-252, https://doi.org/10.1016/j.atmosenv.2014.08.077, 2014.
762  Li, X., Wang, L., Ji, D., Wen, T., Pan, Y., Sun, Y., and Wang, Y.: Characterization of the size-
763  segregated water-soluble inorganic ions in the Jing-Jin-Ji urban agglomeration: Spatial/temporal
764  variability,  size  distribution  and  sources,  Atmospheric  Environment,  77,  250-259,
765  https://doi.org/10.1016/j.atmosenv.2013.03.042, 2013.
766  Li, Y., Tao, J., Zhang, L., Jia, X., and Wu, Y.: High Contributions of Secondary Inorganic Aerosols to
767  PM(2.5) under Polluted Levels at a Regional Station in Northern China, Int J Environ Res Public Health,
768  13, 1202, 10.3390/ijerph13121202, 2016.
769  Liu, B., Wu, J., Zhang, J., Wang, L., Yang, J., Liang, D., Dai, Q., Bi, X., Feng, Y., Zhang, Y., and
770  Zhang, Q.: Characterization and source apportionment of PM2.5 based on error estimation from EPA
771  PMF  5.0  model  at  a  medium  city  in  China,  Environmental  Pollution,  222,  10-22,
772  https://doi.org/10.1016/j.envpol.2017.01.005, 2017a.

Liu, M., Song, Y., Zhou, T., Xu, Z., Yan, C., Zheng, M., Wu, Z., Hu, M., Wu, Y., and Zhu, T.: Fine particle pH during severe haze episodes in northern China, Geophysical Research Letters, 44, 5213-5221, 10.1002/2017gl073210, 2017b.

Liu, Y., Yan, C., Ding, X., Wang, X., Fu, Q., Zhao, Q., Zhang, Y., Duan, Y., Qiu, X., and Zheng, M.: Sources and spatial distribution of particulate polycyclic aromatic hydrocarbons in Shanghai, China, Science of The Total Environment, 584, 307-317, http://dx.doi.org/10.1016/j.scitotenv.2016.12.134, 2017c.

Liu, Y., Yan, C., Feng, Z., Zheng, F., Fan, X., Zhang, Y., Li, C., Zhou, Y., Lin, Z., Guo, Y., Zhang, Y., Ma, L., Zhou, W., Liu, Z., Wei, Z., Dada, L., Dallenbach, K. R., Kontkanen, J., Cai, R., Chan, T., Chu, B., Du, W., Yao, L., Wang, Y., Cai, J., Kangasluoma, J., Kokkonen, T., Kujansuu, J., Rusanen, A., Deng, C., Fu, Y., Yin, R., Li, X., Lu, Y., Liu, Y., Lian, C., Yang, D., Wang, W., Ge, M., Wang, Y., Worsnop , D., Junninen, H., He, H., Kerminen, V. M., Zheng, J., Wang, L., Jiang, J., Petäjä, T., Bianchi, F., and Kulmala, M.: Continuous and Comprehensive Atmospheric Observations in Beijing: A Station to Understand the Complex Urban Atmospheric Environment, Big Earth Data (under review), 10.1080/20964471.2020.1798707, 2020.

Masiol, M., Squizzato, S., Formenton, G., Khan, M. B., Hopke, P. K., Nenes, A., Pandis, S. N., Tositti, L., Benetello, F., Visin, F., and Pavoni, B.: Hybrid multiple-site mass closure and source apportionment of PM2.5 and aerosol acidity at major cities in the Po Valley, Science of The Total Environment, 704, 135287, https://doi.org/10.1016/j.scitotenv.2019.135287, 2020.

Meng, C. C., Wang, L. T., Zhang, F. F., Wei, Z., Ma, S. M., Ma, X., and Yang, J.: Characteristics of concentrations and water-soluble inorganic ions in PM2.5 in Handan City, Hebei province, China, Atmos. Res., 171, 133-146, http://dx.doi.org/10.1016/j.atmosres.2015.12.013, 2016.

Middlebrook, A. M., Bahreini, R., Jimenez, J. L., and Canagaratna, M. R.: Evaluation of Composition-Dependent Collection Efficiencies for the Aerodyne Aerosol Mass Spectrometer using Field Data, Aerosol Sci. Technol., 46, 258-271, 10.1080/02786826.2011.620041, 2012.

Mkoma, S. L., Wang, W., and Maenhaut, W.: Seasonal variation of water-soluble inorganic species in the coarse and fine atmospheric aerosols at Dar es Salaam, Tanzania, Nuclear Instruments and Methods in Physics Research Section B: Beam Interactions with Materials and Atoms, 267, 2897-2902, https://doi.org/10.1016/j.nimb.2009.06.099, 2009.

Ng, N. L., Herndon, S. C., Trimborn, A., Canagaratna, M. R., Croteau, P. L., Onasch, T. B., Sueper, D., Worsnop, D. R., Zhang, Q., Sun, Y. L., and Jayne, J. T.: An Aerosol Chemical Speciation Monitor (ACSM) for Routine Monitoring of the Composition and Mass Concentrations of Ambient Aerosol, Aerosol Sci. Technol., 45, 780-794, 10.1080/02786826.2011.560211, 2011.

Pathak, R. K., Wu, W. S., and Wang, T.: Summertime PM2.5 ionic species in four major cities of China: nitrate formation in an ammonia-deficient atmosphere, Atmospheric Chemistry and Physics, 9, 1711-1722, 2009.

Pye, H. O. T., Nenes, A., Alexander, B., Ault, A. P., Barth, M. C., Clegg, S. L., Collett Jr, J. L., Fahey, K. M., Hennigan, C. J., Herrmann, H., Kanakidou, M., Kelly, J. T., Ku, I. T., McNeill, V. F., Riemer, N., Schaefer, T., Shi, G., Tilgner, A., Walker, J. T., Wang, T., Weber, R., Xing, J., Zaveri, R. A., and Zuend, A.: The acidity of atmospheric particles and clouds, Atmos. Chem. Phys., 20, 4809-4888, 10.5194/acp-20-4809-2020, 2020.

Shi, Z., Vu, T., Kotthaus, S., Harrison, R. M., Grimmond, S., Yue, S., Zhu, T., Lee, J., Han, Y., Demuzere, M., Dunmore, R. E., Ren, L., Liu, D., Wang, Y., Wild, O., Allan, J., Acton, W. J., Barlow, J., Barratt, B., Beddows, D., Bloss, W. J., Calzolai, G., Carruthers, D., Carslaw, D. C., Chan, Q., Chatzidiakou, L., Chen, Y., Crilley, L., Coe, H., Dai, T., Doherty, R., Duan, F., Fu, P., Ge, B., Ge, M., Guan, D., Hamilton, J. F., He, K., Heal, M., Heard, D., Hewitt, C. N., Hollaway, M., Hu, M., Ji, D., Jiang, X., Jones, R., Kalberer, M., Kelly, F. J., Kramer, L., Langford, B., Lin, C., Lewis, A. C., Li, J., Li, W., Liu, H., Liu, J., Loh, M., Lu, K., Lucarelli, F., Mann, G., McFiggans, G., Miller, M. R., Mills, G., Monk, P., Nemitz, E., O'Connor, F., Ouyang, B., Palmer, P. I., Percival, C., Popoola, O., Reeves, C., Rickard, A. R., Shao, L., Shi, G., Spracklen, D., Stevenson, D., Sun, Y., Sun, Z., Tao, S., Tong, S., Wang, Q., Wang, W., Wang, X., Wang, X., Wang, Z., Wei, L., Whalley, L., Wu, X., Wu, Z., Xie, P., Yang, F., Zhang, Q., Zhang, Y., Zhang, Y., and Zheng, M.: Introduction to the special issue "In-depth study of air pollution sources and processes within Beijing and its surrounding region (APHH-Beijing)", Atmos. Chem. Phys., 19, 7519-7546, 10.5194/acp-19-7519-2019, 2019.

Shon, Z.-H., Kim, K.-H., Song, S.-K., Jung, K., Kim, N.-J., and Lee, J.-B.: Relationship between water-soluble ions in PM2.5 and their precursor gases in Seoul megacity, Atmospheric Environment, 59, 540-550, https://doi.org/10.1016/j.atmosenv.2012.04.033, 2012.

Song, S., Gao, M., Xu, W., Shao, J., Shi, G., Wang, S., Wang, Y., Sun, Y., and McElroy, M. B.: Fine-particle pH for Beijing winter haze as inferred from different thermodynamic equilibrium models, Atmos. Chem. Phys., 18, 7423-7438, 10.5194/acp-18-7423-2018, 2018.

Song, S., Nenes, A., Gao, M., Zhang, Y., Liu, P., Shao, J., Ye, D., Xu, W., Lei, L., Sun, Y., Liu, B., Wang, S., and McElroy, M. B.: Thermodynamic Modeling Suggests Declines in Water Uptake and Acidity of Inorganic Aerosols in Beijing Winter Haze Events during 2014/2015–2018/2019, Environmental Science & Technology Letters, 6, 752-760, 10.1021/acs.estlett.9b00621, 2019.

Sun, J., Zhang, Q., Canagaratna, M. R., Zhang, Y., Ng, N. L., Sun, Y., Jayne, J. T., Zhang, X., Zhang, X., and Worsnop, D. R.: Highly time- and size-resolved characterization of submicron aerosol particles in Beijing using an Aerodyne Aerosol Mass Spectrometer, Atmospheric Environment, 44, 131-140, https://doi.org/10.1016/j.atmosenv.2009.03.020, 2010.

Sun, Y., Wang, Z., Dong, H., Yang, T., Li, J., Pan, X., Chen, P., and Jayne, J. T.: Characterization of summer organic and inorganic aerosols in Beijing, China with an Aerosol Chemical Speciation Monitor, Atmospheric Environment, 51, 250-259, https://doi.org/10.1016/j.atmosenv.2012.01.013, 2012.

Sun, Y., He, Y., Kuang, Y., Xu, W., Song, S., Ma, N., Tao, J., Cheng, P., Wu, C., Su, H., Cheng, Y., Xie, C., Chen, C., Lei, L., Qiu, Y., Fu, P., Croteau, P., and Worsnop, D. R.: Chemical Differences Between PM1 and PM2.5 in Highly Polluted Environment and Implications in Air Pollution Studies, Geophysical Research Letters, 47, e2019GL086288, 10.1029/2019gl086288, 2020.

Takami, A., Miyoshi, T., Shimono, A., Kaneyasu, N., Kato, S., Kajii, Y., and Hatakeyama, S.: Transport of anthropogenic aerosols from Asia and subsequent chemical transformation, Journal of Geophysical Research, 112, 10.1029/2006JD008120, 2007.

Tian, M., Wang, H., Chen, Y., Zhang, L., Shi, G., Liu, Y., Yu, J., Zhai, C., Wang, J., and Yang, F.: Highly time-resolved characterization of water-soluble inorganic ions in PM2.5 in a humid and acidic mega city in Sichuan Basin, China, Science of The Total Environment, 580, 224-234, https://doi.org/10.1016/j.scitotenv.2016.12.048, 2017.

Wang, S., Yin, S., Zhang, R., Yang, L., Zhao, Q., Zhang, L., Yan, Q., Jiang, N., and Tang, X.: Insight into the formation of secondary inorganic aerosol based on high-time-resolution data during haze episodes and snowfall periods in Zhengzhou, China, Science of The Total Environment, 660, 47-56, https://doi.org/10.1016/j.scitotenv.2018.12.465, 2019.

Wang, S., Wang, L., Li, Y., Wang, C., Wang, W., Yin, S., and Zhang, R.: Effect of ammonia on fine-particle pH in agricultural regions of China: comparison between urban and rural sites, Atmos. Chem. Phys., 20, 2719-2734, 10.5194/acp-20-2719-2020, 2020.

Wang, Y., Zhang, Q., Jiang, J., Zhou, W., Wang, B., He, K., Duan, F., Zhang, Q., Philip, S., and Xie, Y.: Enhanced sulfate formation during China's severe winter haze episode in Jan 2013 missing from current models, Journal of Geophysical Research: Atmospheres, 119, 10.1002/2013JD021426, 2014.

Weber, R. J., Guo, H., Russell, A. G., and Nenes, A.: High aerosol acidity despite declining atmospheric sulfate concentrations over the past 15 years, Nature Geoscience, 9, 282-285, 10.1038/ngeo2665, 2016.

Wongphatarakul, V., Friedlander, S. K., and Pinto, J. P.: A comparative study of PM2.5 ambient aerosol chemical databases, Environmental Science and Technology, 32, 3926-3934, 10.1021/es9800582, 1998.

Xu, Q., Wang, S., Jiang, J., Bhattarai, N., Li, X., Chang, X., Qiu, X., Zheng, M., Hua, Y., and Hao, J.: Nitrate dominates the chemical composition of PM2.5 during haze event in Beijing, China, Science of The Total Environment, 689, 1293-1303, https://doi.org/10.1016/j.scitotenv.2019.06.294, 2019a.

Xu, W., Liu, X., Liu, L., Dore, A. J., Tang, A., Lu, L., Wu, Q., Zhang, Y., Hao, T., Pan, Y., Chen, J., and Zhang, F.: Impact of emission controls on air quality in Beijing during APEC 2014: Implications from water-soluble ions and carbonaceous aerosol in PM2.5 and their precursors, Atmospheric Environment, 210, 241-252, https://doi.org/10.1016/j.atmosenv.2019.04.050, 2019b.

Xue, J., Lau, A. K. H., and Yu, J. Z.: A study of acidity on PM2.5 in Hong Kong using online ionic chemical composition measurements, Atmospheric Environment, 45, 7081-7088, https://doi.org/10.1016/j.atmosenv.2011.09.040, 2011.

Yao, X., Yan Ling, T., Fang, M., and Chan, C. K.: Comparison of thermodynamic predictions for in situ pH in PM2.5, Atmospheric Environment, 40, 2835-2844, https://doi.org/10.1016/j.atmosenv.2006.01.006, 2006.

Yu, X.-C., He, K.-B., Yang, F., Yang, F.-M., Duan, F.-K., Zheng, A.-H., and Zhao, C.-Y.: Application of ion chromatography to the determination of water-soluble inorganic and organic ions in atmospheric aerosols, Journal of environmental sciences (China), 16, 813-815, 2004.

Yue, F., Xie, Z., Zhang, P., Song, S., He, P., Liu, C., Wang, L., Yu, X., and Kang, H.: The role of sulfate and its corresponding S(IV)+NO2 formation pathway during the evolution of haze in Beijing, Science of The Total Environment, 687, 741-751, https://doi.org/10.1016/j.scitotenv.2019.06.096, 2019.

Zhang, B., Zhou, T., Liu, Y., Yan, C., Li, X., Yu, J., Wang, S., Liu, B., and Zheng, M.: Comparison of water-soluble inorganic ions and trace metals in PM2.5 between online and offline measurements in Beijing during winter, Atmospheric Pollution Research, 10, 1755-1765, https://doi.org/10.1016/j.apr.2019.07.007, 2019.

Zhang, J. K., Cheng, M. T., Ji, D. S., Liu, Z. R., Hu, B., Sun, Y., and Wang, Y. S.: Characterization of submicron particles during biomass burning and coal combustion periods in Beijing, China, Science of The Total Environment, 562, 812-821, https://doi.org/10.1016/j.scitotenv.2016.04.015, 2016.

Zhang, Q., Jimenez, J. L., Worsnop, D. R., and Canagaratna, M.: A Case Study of Urban Particle Acidity and Its Influence on Secondary Organic Aerosol, Environ. Sci. Technol., 41, 3213-3219, 10.1021/es061812j, 2007.

Zhao, J., Zhang, F., Xu, Y., and Chen, J.: Characterization of water-soluble inorganic ions in size-segregated aerosols in coastal city, Xiamen, Atmos. Res., 99, 546-562, http://dx.doi.org/10.1016/j.atmosres.2010.12.017, 2011.

Zhou, Y., Xue, L., Wang, T., Gao, X., Wang, Z., Wang, X., Zhang, J., Zhang, Q., and Wang, W.: Characterization of aerosol acidity at a high mountain site in central eastern China, Atmospheric Environment, 51, 11-20, https://doi.org/10.1016/j.atmosenv.2012.01.061, 2012.

Ziemba, L. D., Fischer, E., Griffin, R. J., and Talbot, R. W.: Aerosol acidity in rural New England: Temporal trends and source region analysis, Journal of Geophysical Research: Atmospheres, 112, 10.1029/2006jd007605, 2007.

Zou, J., Liu, Z., Hu, B., Huang, X., Wen, T., Ji, D., Liu, J., Yang, Y., Yao, Q., and Wang, Y.: Aerosol chemical compositions in the North China Plain and the impact on the visibility in Beijing and Tianjin, Atmos. Res., 201, 235-246, https://doi.org/10.1016/j.atmosres.2017.09.014, 2018.